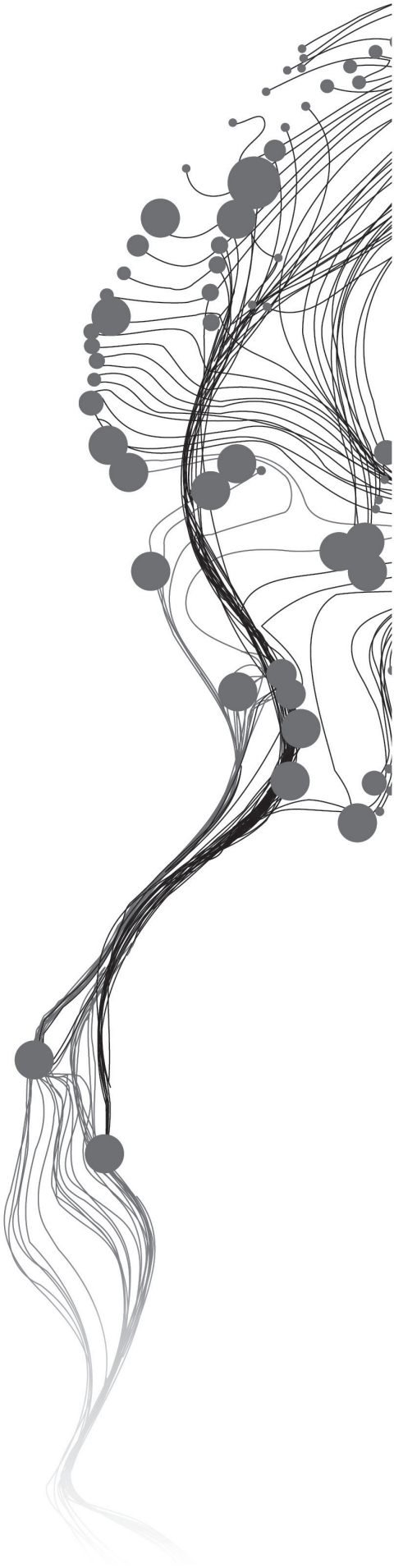# STOCHASTIC GEOMETRY FOR RADAR SPECKLE CHARACTERIZATION

MEAZA ABERA FUFA
March, 2012

SUPERVISORS:

Prof. Dr. Ir. Alfred Stein
Dr. Valentyn Tolpekin

STOCHASTIC GEOMETRY FOR RADAR SPECKLE CHARACTERIZATION

MEAZA ABERA FUFA
Enschede, The Netherlands, March, 2012

Thesis submitted to the Faculty of Geo-information Science and Earth Observation of the University of Twente in partial fulfilment of the requirements for the degree of Master of Science in Geo-information Science and Earth Observation.
Specialization: Geoinformatics

ABSTRACT

Speckle is a problem to Synthetic Aperture Radar image analysis. Spatial point pattern analysis is applied to characterize the spatial pattern of radar speckle. Forest, agriculture and urban land-use classes are selected from ERS-2 SAR image of Overijssel and Gelderland provinces of Netherlands to study the spatial pattern of speckle. Analyzing the spatial pattern of speckle helps to choose point process model which describes the process and also may help to develop filter for speckle reduction. The gamma probability distribution of intensity is applied to separate strong reflectors such as corner reflectors and metal objects from the data. The homogeneous F, G, J and K functions are used to study the spatial pattern of the speckle. A clustered pattern of speckle is observed in the three land-use classes by comparing the observed distance functions to the theoretical Poisson distribution. A strong clustered pattern of speckle is observed in the selected agricultural area in the analysis carried on both bright and dark speckle. The analysis procedure is also applied in ALOS PALSAR SAR image of Nairobi city. A clustered pattern of speckle is also observed in subset park area Nairobi city SAR image.

Keywords

Speckle; SAR; Nearest-neighbor distances; Ripley's K-function; Spatial point pattern; Strong reflectors

ACKNOWLEDGEMENTS

TABLE OF CONTENTS

LIST OF FIGURES

LIST OF TABLES

Chapter 1

Introduction

1.1 MOTIVATION

Synthetic aperture radar (SAR) is a form of radar which produces high resolution imagery of the earth's surface in all weather condition. SAR sensors are active systems, providing their own illumination source, and they operate in the microwave region of the electromagnetic spectrum. The microwave signal can penetrate vegetation canopy and some distance into the surface coverage depending on the wavelength used in the imaging system. These features have made SAR imaging a practical choice for environmental monitoring. However, SAR images contain multiplicative noise, which is called speckle [20]. The speckle makes interpretation of SAR image more complicated than optical image. Speckles occur by random interferences, either constructive or destructive, between electromagnetic waves from different reflections in the imaged area of resolution cell [13]. Speckle degrades the quality of SAR images, and it is often necessary to enhance the image by speckle filtering prior to image interpretation, analysis or classification. A speckle suppression filter should filter the homogeneous areas with reasonable speckle reduction capability and for these speckle pattern should be considered in filter selection [24]. Since speckle reduces the ability to extract information from SAR images, specialized techniques are required to deal with such imagery.

Since speckle is the result of interactions between scatterers inside ground resolution cell at the sub pixel level, the speckle pattern may reflect the condition of ground surface. Some studies [17, 19] have been carried out to extract information by analyzing speckle pattern. Under certain conditions, speckle may also contain information on the geometrical arrangement of scatterers at the sub-resolution cell level. Those detail of arrangement are not directly perceivable from radar imagery or the associated raw data, but may be revealed, to some extent, through a proper analysis of the speckle.

Some studies [17, 19] have shown that it is possible to extract beneficial information from the speckle pattern. Even if these studies show the benefit of analyzing speckle, speckle is a problem to image visualization, analysis and classification. The presence of speckle in images hides the spatial patterns of surface features and decreases the detect ability of ground targets. Extensive work has been carried out for the reduction of speckle [8, 16, 12, 28]. Sheng and Xia [24]evaluated radar speckle suppression filters available in Erdas imaging radar module based on speckle suppression index, edge enhancing, feature preserving index, image preserving coefficient and speckle image analysis criteria. They described that speckle pattern should be considered in filter selection as close relationship is noticed between the filters performance and speckle patterns in the study. Many studies [14, 18] have been done to remove noise and preserve all textural features in the SAR images.

Some studies have been done in the statistical analysis of speckle. A study is carried out to model partially developed speckle in medical ultra sound image using a doubly stochastic compound poisson point process [6]. The study shows that the probability density function approaches an exponential distribution when the mean number of scatterers in a resolution cell is

increased and this is consistent with fully developed speckle noise as demonstrated by the Central Limit theorem. Ouchi [21] investigated the autocorrelation functions of SAR speckle when the scatterers are stationary and in random motion, concluding that the speckle correlation depends strongly on random motion in the region of small decorrelation time. Statistical characterization and modeling of SAR image using the K distribution has been done by [5]. But none of these studies have analyzed the spatial pattern of speckle.

One approach to analyze patterns observed in images is spatial point pattern analysis. Stein et al [26] has mentioned that there is a possibility of analyzing radar speckle using spatial point pattern analysis. Stochastic geometry and spatial statistics are important tools to analyze random spatial patterns in many modern branches of physics, material sciences, biology and environmental sciences. They offer successful models for the description of process which generate random spatial patterns. Spatial point pattern analysis can be used for characterizing observed patterns in the field of stochastic geometry. The use of spatial point-process analysis as an aid to describe topsoil lead distribution in urban environments has been explored by [29]. Perry et al [22] have described a range of methods for the description and analysis of spatial patterns in plants. Stein and Georgiadis [25] have studied the spatial distribution of the most abundant herd species in Laikipia, cental Kenya using spatial point pattern analysis. Lu [17] has also studied the spatial temporal pattern associated with a new forest disease using spatial point process methodology. Analysis of the earthquake data considering it as point pattern and the application of the Strauss point process method has been studied in [1].

The spatial point pattern analysis method is powerful in dealing with events occurring randomly on earth. Radar speckle can be considered as random phenomena that occur during radar imaging system. Pixels which have extreme value can be treated as random variables so it is possible to apply spatial point pattern analysis approach in order to analyze the speckle pattern. Such an approach helps to understand radar speckle and to choose point process model which describes the process. This further may also help to develop filter for speckle reduction. In this study, analysis on SAR image is carried out considering the speckle as point pattern; if there is a tendency of the speckle pattern to exhibit a systematic pattern over an area as opposed to being randomly distributed.

1.1.1 Objectives

The general objective of the study is to analyze and characterize the spatial pattern of radar speckle. The specific objectives of the study are

1. Distinguish speckled pixels

2. generate point pattern of speckles

3. Analyze the intensity of speckles

4. Analyze the spatial distribution of the speckles using homogeneous F, G, J and K function

1.1.2 Research questions

1. Are all bright pixels in SAR image resulted from speckle?

2. Which threshold value is used to select pixels which have higher brightness value?

3. Does speckle pattern exhibit clustering or regularity?

4. Is there a relationship between speckle pattern and land cover type?

Chapter 2

Radar Speckle

2.1 THE SAR SYSTEM

SAR systems operate in the microwave region of the electromagnetic spectrum at wavelengths that propagate with no hinderance through atmosphere and clouds. The microwave also penetrate some distance into the surface coverage. The penetration depend on the type of wavelength used. Table 2.1 shows the wavelength bands commonly used in imaging radar systems. SAR system with longer wavelength can penetrate vegetation and soil.

Table 2.1 Wavelengeths used in SAR imaging system

Band	Usual wavelength
P-band	65cm
L-band	23cm
S-band	10cm
C-band	5cm
X-band	3cm
K-band	1.2cm

SAR systems can transmit vertical(V) or horizontal(H) polarized waves and can also receive horizontal or vertical return signals. When the electric field is transmitted and received in the same polarization, it is called like-polarized(HH or VV). When it is transmitted in the horizontal direction and received in the vertical or vice versa, it is called cross-polarized(HV or VH). The horizontal and vertical arrangement of the electric field is shown in Figure 2.1. The electric field vector is always perpendicular to the magnetic field.
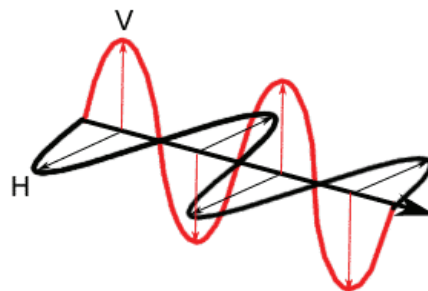
Figure 2.1: Vertical and Horizontal polarization of radar EM wave.

2.2   SCATTERING MECHANISMS

SAR measures the scattering of incident energy from scatterers. Figure 2.2 shows common scattering mechanisms that occur in SAR imaging. Bright pixels in the image can be observed due to double bounce of the return signals by corner reflectors especially in city area. The planar building sides intersect the surrounding ground at a right angle, creating a corner reflector as shown in Figure 2.2. Due to the corner reflectors, a strong signal is directed back toward the radar antenna regardless of the depression angle. Metal objects such as powerline towers and bridges appear very bright in radar images. The presence of moisture in soil, snow and vegetation increases their dielectric constant and this increases their radar reflectivity. If there are buildings in the agricultural field, bright pixels are also observed in the image.
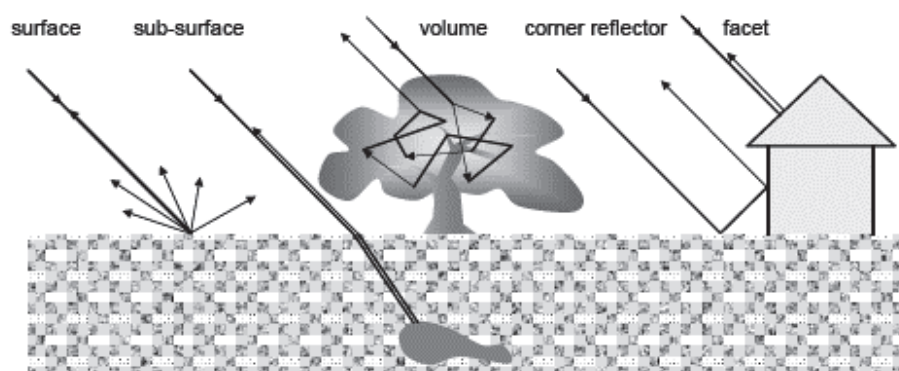
Figure 2.2: Common scattering mechanisms. Source: [23]

Smooth surface such as water appear dark in the radar image because flat surfaces reflect little or no energy back to the radar as shown in Figure 2.3. The back scattering of the radar signal depend on the imaging process such as the wavelength of the radar signal, the polarization and the incident angle used in the imaging process. The volume of the feature, the moisture content and the dielectric nature of the surface also affect the back scattering of the radar signal. Generally a bright pixel represent a large amount of energy is backscattered to the radar signal and a dark pixel represent a small amount of energy is backscattered to the radar signal.
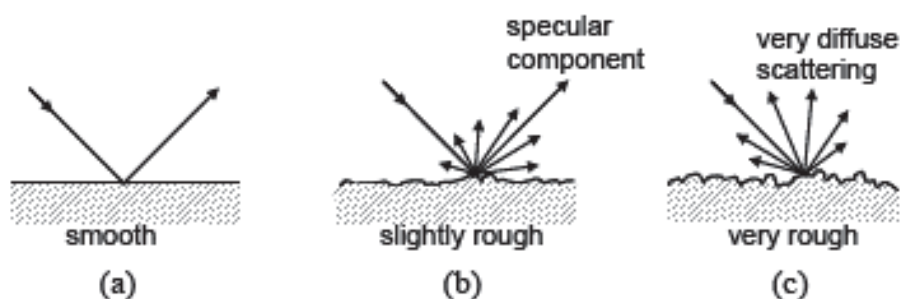
Figure 2.3: Depicting the trend to diffuse surface scattering as roughness increases. Source: [23]

2.3   SPECKLE OCCURRENCE

SAR image shows the estimate of the return signal for target in the ground. The total amplitude at a resolution cell is regarded as resulting from the sum of contributions from many elementary scatterers in the resolution cell [15]. Figure 2.4 shows the distribution of N individuals phasors within a resolution cell in part A, all phasors translated to the same origin in part B, the phasors sum of all scatterers in part C of the image.
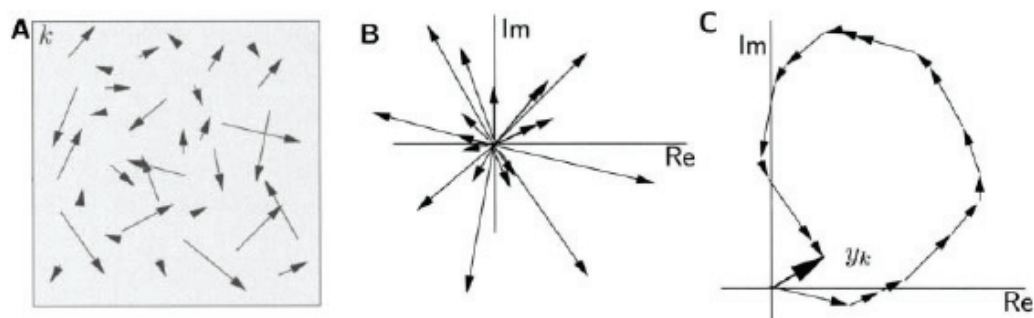
Figure 2.4: Summation of scatterers with in resolution cell k. Source: [15].

In coherent imaging system such as synthetic aperture radar image, laser, and ultrasound image, salt and pepper appearance in the image is observed. Interference of the dephased return signals from scatterers with in one resolution cell create the salt and pepper appearance of the image known as speckle. The speckle pattern appears in the image as bright pixels where the interference is highly constructive, dark pixels where the interference is highly destructive and all values in between [13]. As shown in Figure 2.5 constructive interference indicates the increase in the amplitude of the return signals when multiple return signals from scatters of equal frequency are transmitted precisely in phase. On the other hand destructive interference indicates the decrease in the amplitude of the return signals when the return signals from scatterers are transmitted out of phase. In radar image if the size of the scatterers is much much greater than the wave length those features are considered as scatterers. If there are many scatterers with in one resolution cell fully developed speckle will be created, if there are few scatterers less than 10 or 20, partially developed speckle is created [6].
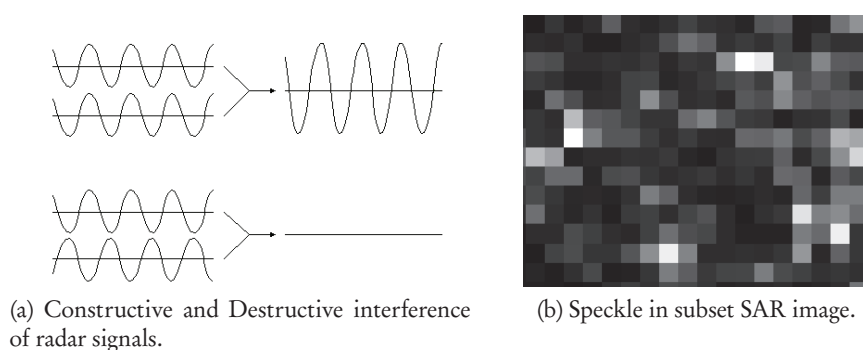
(a) Constructive and Destructive interference of radar signals.

(b) Speckle in subset SAR image.

Figure 2.5: Interference of radar signals and Speckles in subset SAR image.

2.4   STATISTICS OF SPECKLE

Due to difficulty encountered to describe the the response of individual scatterers within a resolution cell, the property of speckle pattern can be described by the probability distribution of the intensity.

Speckle in a single look intensity image has an exponential distribution [20]:

$$P(I) = (I/2\sigma^2) \exp(-I/2\sigma^2) \tag{2.1}$$

with mean value and standard deviation both equal to $2\sigma^2$, where σ is the average value of the intensity measured by sensors, called average radar reflectivity [5]. Speckle in multilook intensity image is described by a Gamma probability distribution [20]:

$$P_k(I) = \frac{k^k}{(2\sigma^2)^k \tau(k)} I^{k-1} \exp\left(-\frac{kI}{2\sigma^2}\right) \tag{2.2}$$

Where $\tau(.)$ is the Gamma function. $2\sigma^2$ and $(2\sigma^2)/(k)^{1/2}$ represent its mean and standard deviation respectively. The mean (M) to standard deviation (Sd) ratio of the Gamma distribution gives

$$(\frac{M}{Sd})^2 = k = constant \tag{2.3}$$

Equation 2.3 is known as the equivalent number of looks (ENL). ENL is used to estimate the speckle noise in a SAR image and is calculated by taking homogeneous area from the image [9].

Chapter 3

Data

This chapter provides description of the type of radar image used, the selected study area, the land-use classes and the softwares used for the analysis. Figure 3.1 shows the study area of this research.
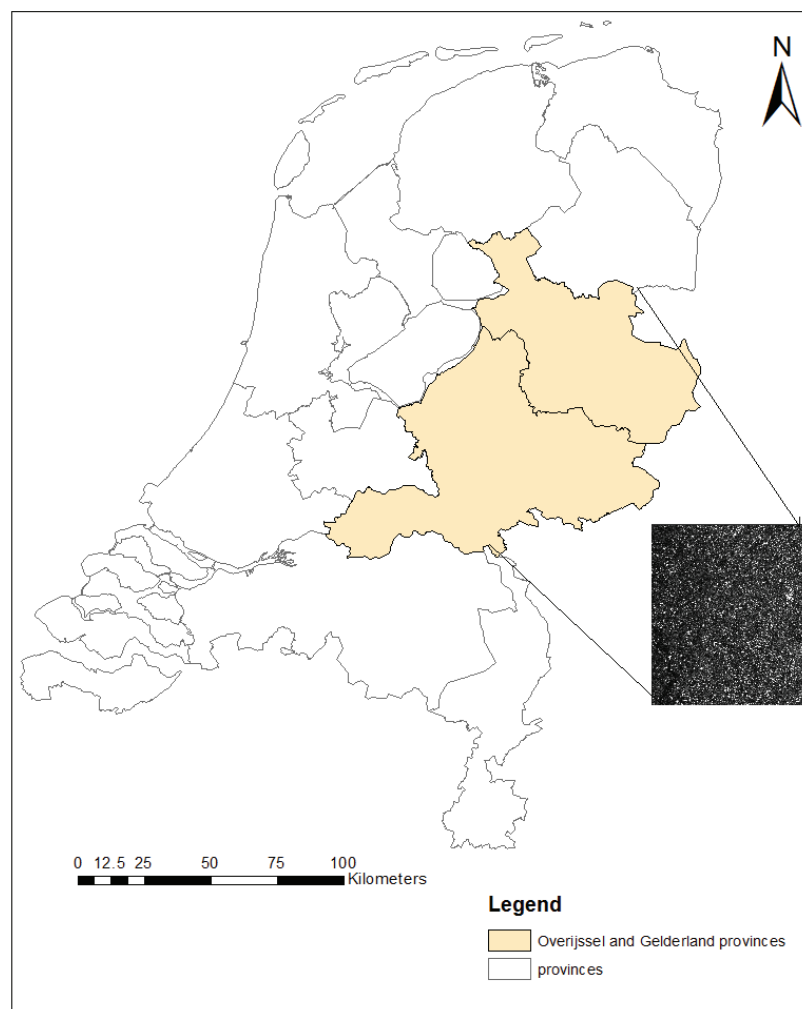
Figure 3.1: Study Area and Radar Image of the study area

3.1   DATA SET AND STUDY AREA

The original radar image used in this study is single look complex SAR image. The image is taken by ERS-2 satellite and include C-band SAR operating with vertical-vertical(VV) polirization. The

image was taken in November 2002. The C-band has wavelength range between 3.8 and 7.5 cm. Most of the time 6 cm wavelength is used. Imaging radar equipped with C-band are generally not hindered by atmospheric effects and are capable of 'seeing' through tropical clouds and rain showers. Its penetration capability with regard to vegetation canopies or soils is limited and is restricted to the top layers. Radar polarization refer to the orientation of the electric field in the electromagnetic field in imaging radar system. Most of the time vertical or horizontal polarization are used. This means that the electric field of the wave is in a vertical plane or in a horizontal plane. The radar image used for this study has VV polarization which means vertical transmit and vertical receive of the electromagnetic field is used to detect the objects. The reflection from an object depends on the type of polarization used and the geometry of the object. The image has azimuth spacing of 4m and range spacing of 20m. The image has 2500 by13647 pixel dimension. It covers most part of Overijssel and Gelderland provinces of Netherlands(Figure 3.1).

3.2   DATA PREPARATION AND PROCESSING

The original image is single look SAR image. In the single look image the the resolution in the range and azimuth direction are not equal. The single look image has azimuth spacing of 4m and range spacing of 20m, visualization of the different features is difficult. Since the the resolution in the range and azimuth direction are not equal it affects the result of distance function calculation. For better visualization and accurate distance measurement the single look image is changed into multi-look (5 look) Figure 3.2. The multi look image has 20m by 20 m resolution cell. For the image to correctly represent the surface, the slant range measurement is corrected to ground range.

(a)   (b)
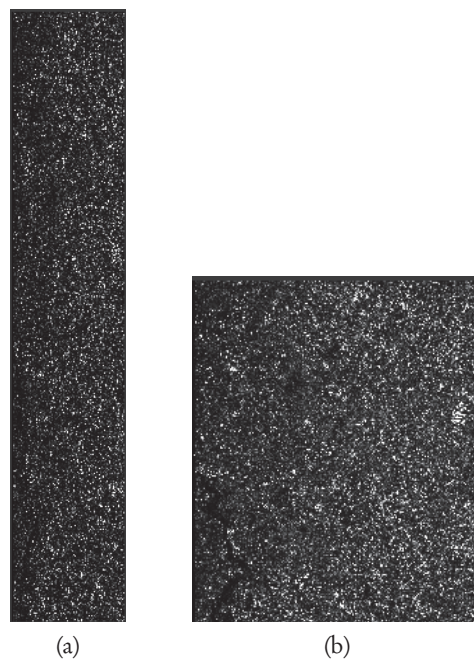
Figure 3.2: SAR image of the study area (a)single-look image (b)Multilook image.

3.2.1 Selection of land-use classes

After preprocessing of the data three land-use classes are selected to characterize the speckle pattern in the radar image. The land-use classes are forest, agriculture and urban. For each land-use class 100 by 100 pixel dimension subset image is used. Two subset images are taken for each land-use class from the multi-look radar image with the support of google map. Subset images from Hengelo city is taken for urban land use class. Subset image for forest area is taken from forest found around Hellendoorn city. Subset agricultural area image is taken from agricultural areas found around Hengelo city. Most of the agricultural areas in Netherlands have buildings in between the field. So it is difficult to get homogeneous agricultural field in the study area. The optical and SAR image of the subset land-use classes are shown in Figures 3.3 and 3.4 respectively.

(a)	(b)	(c)

Figure 3.3: Optical image of subset land-use classes (a) Forest area (b) agricultural area (c) urban area.

(a)	(b)	(c)
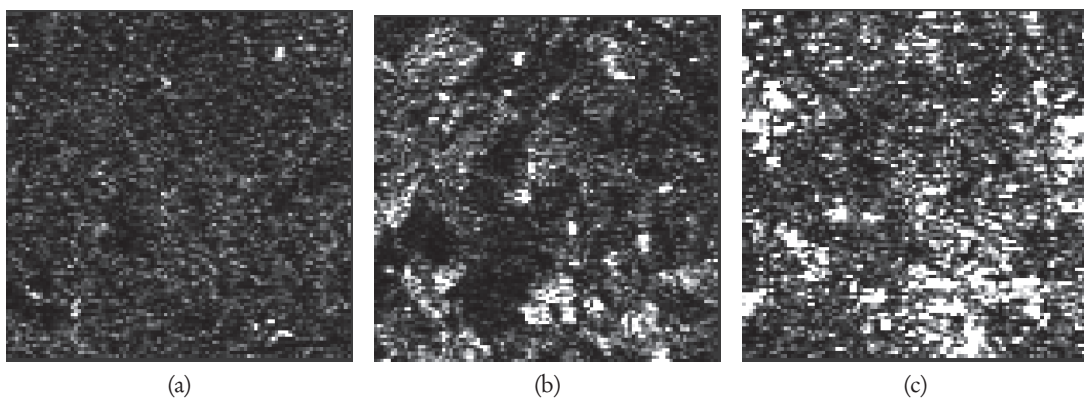
Figure 3.4: SAR image of subset land-use classes (a) Forest area (b) agricultural area (c) urban area.

Park area land -use class is selected from HH polarization ALOS PALSAR image of Nairobi city to test the analysis procedure(Figure 3.5). The park area is almost free of strong reflectors. The subset image has 100 by 100 pixel dimension. The resolution of the image is 6.5m by 6.5m. The image is taken in January 2006.

(a)   (b)
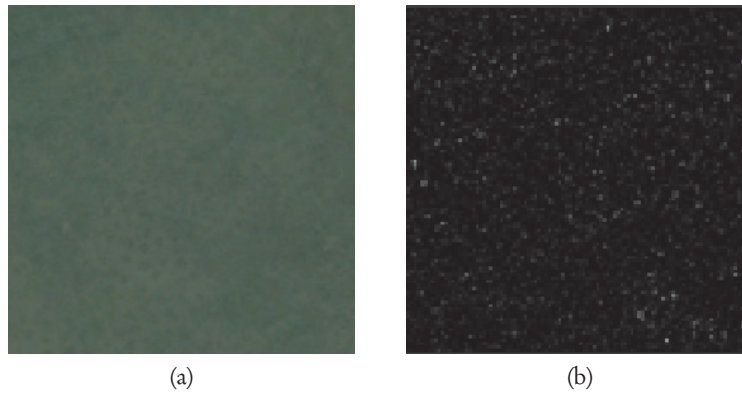
Figure 3.5: (a)Subset optical image of park area; (b) Subset SAR image of park area.

3.2.2 software

Nest software is used to visualize the radar image, to change the single-look original image to multi-look image, to change the slant range measurement to ground range, to take subset image of the different land-use classes and change the pixel value to text file.

Spatstat package in R language is used to analyze the point pattern. The spatstat package has capability of generating point pattern of data, doing summary statistics, fitting the point pattern data to a spatial point process model and visualizing the pattern [3].

Chapter 4

Spatial point pattern

4.1 SPATIAL POINT PROCESS

Spatial point process is a stochastic mechanism which generate spatial point pattern [7]. A spatial pattern generated from a spatial point process is termed as a realization of the process [10]. The points in a pattern are called events. The main property of spatial point process is its intensity which is the number of events per unit area. To explain different point process, the complete spatial randomness (CSR) is used as a base. In complete spatial randomness, the events follow the poisson distribution in the region and the events don't interact in the region [7].

To study the spatial patterns of points first we have to differentiate between stationary and non stationarity point process. Stationary point process are process which are invariant under translation and have constant intensity over the area under study. In non stationary point process the spatial patterns follow spatial trend. Point processes can also be described in terms of their isotropy that means they are invariant under rotation.

Spatial point patterns can be characterized based on their first-order and second-order properties. First order property is based on the density of points using quadrat count and kernel estimation. The first-order property shows only the intensity variation. The second order property characterization is based on nearest neighbor distance and the K function.

4.2 DENSITY BASED POINT PATTERN ANALYSIS

In exploratory analysis the variation of intensity of point pattern over an area is studied using quadrant count and kernel estimation. Quadrat count exploratory analysis is carried out by dividing the study area into subregions and counting the number of events in each subregion. Quadrat count analysis is a measure of dispersion, and not really pattern, because it is based primarily on the density of points, and not their arrangement in relation to one another.

The kernel is a mathematical function that calculates how the surface value decreases as it reaches the radius. The resulting intensity surface can be influenced by the type of kernel used and the bandwidth. There are different kinds of kernel functions. The gaussian kernel is used in spatstat package to draw the intensity map of the point pattern. In kernel estimate results are sensitive to change in bandwidth. When bandwidth is large, the intensity appear smooth and local details obscured. When the bandwidth is small, the intensity appears as local spikes at event locations. The best bandwidth can be selected based on prior information about underlying spatial process and by comparing the result obtained from various bandwidths.

4.3 DISTANCE BASED POINT PATTERN ANALYSIS

Distance between events in a point pattern analysis can be quantified by using summary statistics. If the data contains non-stationary point process, Kinhom (an inhomogeneous version of k function [4]) and inhomogeneous J-function [27] are applied. For stationary point process the

the homogeneous nearest neighbor distance F, G, J and K functions are used to analyze the distance between events and also point to event distances [7, 2]. In a stationary point process the G-function provides the cumulative distribution function of all event-to-nearest-event distances. The empirical distribution function of the observed nearest neighbor distance is given as:

$$G(r) = \frac{1}{n(x)} \sum_i 1\{t_i \leq r\} \tag{4.1}$$

For a homogeneous poisson point process of intensity λ, the G- function can be given as

$$G_{pois}(r) = 1 - \exp(-\lambda \Pi r^2) \tag{4.2}$$

Observed events are then tested for departure from the poisson distribution. There are three general patterns random, uniform and clustered. In random pattern any point is equally likely to occur at any location and the position of any point is not affected by the position of any other point. In uniform distribution every point is as far from all of its neighbors as possible. In clustered pattern, many points are concentrated close together and large areas that contain very few, if any, points. A clustered distribution has a G-function higher than the G-function for a homogeneous poisson process, whereas a regular pattern has a G-function below the G-function for the homogeneous poisson process.

Distance between a randomly chosen point at location x and its nearest neighbor event can be analyzed using the F function. The empirical distribution function of all j point to nearest event distances can be calculated as

$$F(r) = \frac{1}{m} \sum_j 1\{d(u_j, x) \leq r\} \tag{4.3}$$

For a homogeneous poisson process the F function is defined as

$$F_{pois}(r) = 1 - \exp(-\lambda \Pi r^2) \tag{4.4}$$

A regular distribution has a F-function higher than the F-function for a homogeneous poisson process, whereas a clustered pattern has a F-function below the F-function for the homogeneous poisson process. The ratio of the G function and the F function is given by a J function

$$J(r) = \frac{1 - G(r)}{1 - F(r)} \tag{4.5}$$

A J function has advantage when no reference is required for the intensity of some Poisson process [11]. For a homogeneous poisson process, $F_{pois} = G_{pois}$, so that

$$J_{pois}(r) = 1 \tag{4.6}$$

values $J(r)$ exceeding 1 suggest a regular pattern, and $J(r)$ less than 1 suggest a clustered pattern. K function calculates the the relative number of events at distance d calculated around all events. K function looks at information beyond the nearest neighbors. The K function can be given as

$$K(r) = \frac{1}{\lambda} E[n(X \cap b(u, r) \setminus \{u\} | u \epsilon X] \tag{4.7}$$

K function for the homogeneous poisson process is given as

$$K_{pois}(r) = \Pi r^2 \tag{4.8}$$

A clustered distribution has a K-function higher than the K-function for a homogeneous poisson process, whereas a regular pattern has a K-function below the K-function for the homogeneous poisson process. The estimation of distance functions is restricted by edge effects because there are events outside the window which may have influence in the distribution of the pattern. An edge correction is required to reduce the bias of the distance function measurement.

Chapter 5

Methodology

The methodology followed to analyze the speckle pattern is shown in Figure 5.1.
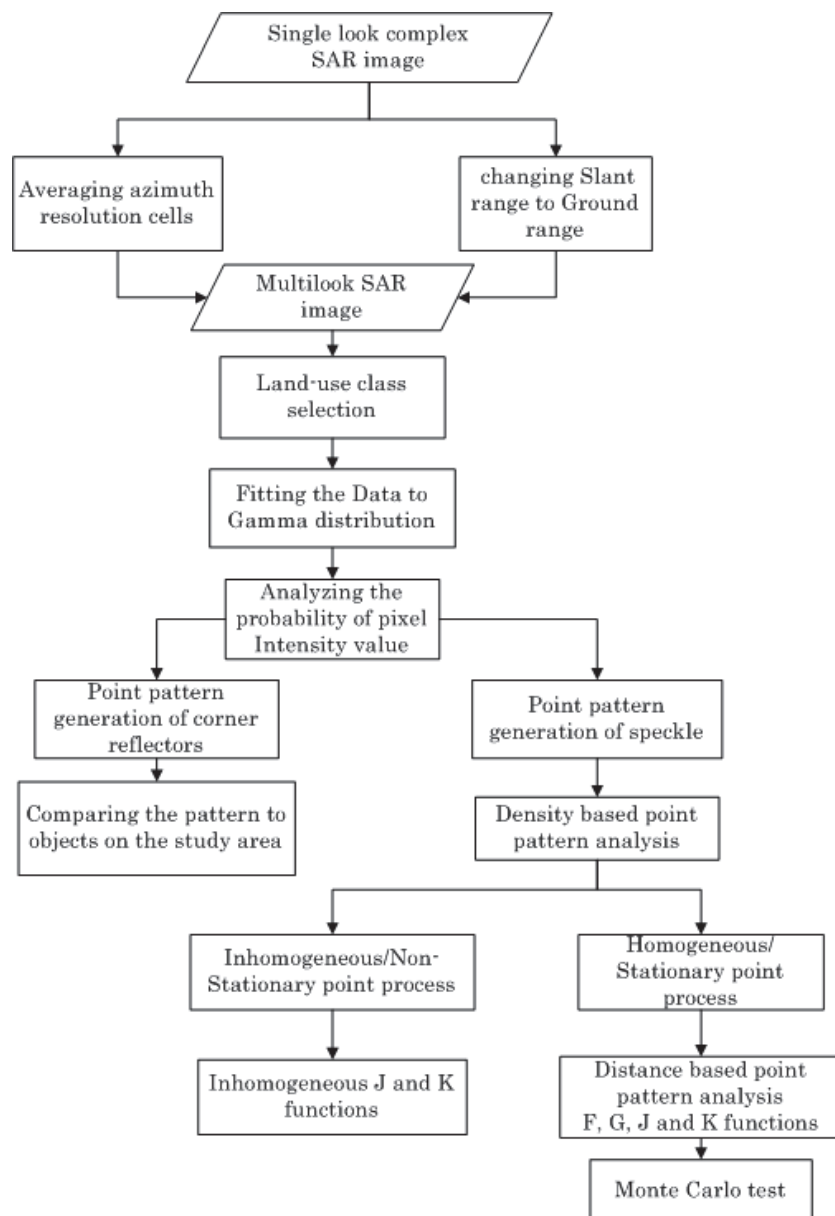
Figure 5.1: Methodology flow chart.

This chapter describes the methodology that has been used to achieve the objective of the

research. The methodology that has been used to characterize the radar speckle is the spatial point pattern analysis. The speckles have been considered as events occurring in the study area and the spatial pattern of the speckles has been studied. The study area has been explored using land use map of the study area and optical image of the study area. Land-use classes of urban, agriculture and forest has been selected. Fitting a gamma distribution to the different land-use class has been done to isolate strong reflectors from speckle since all bright pixels are not due to speckle. Outliers/ strong reflectors from the data are removed which are unlikely to occur above a certain intensity value based on the probability distribution analysis.

Pixels which have higher and lower intensity value are then isolated from other pixels to generate the point pattern. The kernel estimation (Gaussian kernel in spatstat package) is used to show the intensity map of the area, the place where there is high or low intensity. Based on the intensity map of the point pattern the stationary point pattern analysis is selected. To analyze the event to nearest event distance the G function is used. To analyze point to nearest event distance the F function is used. To analyze event to event distances the k function is used. The graph of the functions tell us whether the points are clustered or regularly distributed by comparing the result with the theoretical Poisson graph [7, 2]. The Monte Carlo test is used to test the the departure of the observed distance functions from the theoretical poisson process. The steps followed in characterizing the spatial patterns of the speckles is as follows.

5.1 FITTING GAMMA DISTRIBUTION TO THE INTENSITY HISTOGRAM

Pixels intensity value which are unlikely to occur in the the subset images are removed from the data by integrating the density curve of the gamma distribution. In R package, it is possible to draw the Gamma distribution of the radar intensity. As expressed in the R help manual, the Gamma distribution with parameters shape=a and scale=s has the following density :

$$f(x) = \frac{1}{s^a \tau(a)} x^{a-1} \exp\left(-\frac{x}{s}\right) \tag{5.1}$$

for $x \geq 0$, $a > 0$ and s >0. The function dgamma is used to draw the density for the gamma distribution with parameter shape and scale. To draw the gamma distribution for the multi look radar image, the equivalent number of looks (ENL) is used as shape parameter and the reciprocal of the ENL is used as scale parameter by comparing equation 5.1 and equation 2.2. The ENL in the multilook radar image is different from the ENL obtained from the radar processor and can be calculated by taking homogeneous area from the image. The ENL is calculated by dividing mean of the intensity of the subset image by the standard deviation of the intensity of the subset image as shown in equation 2.3.

Taking a homogeneous forest area 40 by 40 pixel dimensions, ENL value of 3.6 is obtained. But a better fit is visualized when ENL value of 4.3 is used as shape parameter. In the study area to get homogeneous area is difficult to calculate the ENL of the image. Experiments are done using ENL value 3.6, 4.3 and 5. ENL value 4.3 is selected to fit the gamma distribution to the data which is found in between ENL value 3.6(from calculation) and 5(from the radar processor).

The function pgamma is used in R package to calculate the probability distribution function of the intensity. It is also possible to calculate the probability of getting a certain pixel with in some intensity interval by integrating the density function.

The intensity of the radar image for each land-use class is normalized by dividing the intensity by the average intensity of each land-use class. Normalizing the intensity of each land-use class by the average intensity decrease the the variation of the intensity with in the land-use classes, helps to properly fit the the distribution curve to the histogram of the intensity and to compare the result obtained from the different land-use classes.

5.2   POINT PATTERN GENERATION OF SPECKLE

All pixels which are highly bright are not speckled pixels. As explained in Section 2.2 bright pixels can be seen in the image due to strong reflectors especially in city areas. As explained in section 5.1 probability distribution analysis is used to isolate strong reflectors from the data. After strong reflectors are isolated from the data speckled pixels are taken from the data by assuming one percent of the highest intensity pixel value as speckled pixels. Again the same procedure is followed with a different assumption that is five percent of the highest intensity pixel value as a speckled pixel. After experiments have done in the different assumptions, the one percent of the highest intensity value is used to report in the result chapter of this study. One percent of the highest intensity value in the data can be a sample of the speckled pixels for each land use-class even if the exact number of speckled pixels in the data are not known. The term bright speckles is used in this study to represent bright pixels resulted from highly constructive interference of return signals from scatterers with in one resolution cell. Dark speckles is used in this study to represent dark pixels resulted from highly destructive interference of return signals from scatterers with in one resolution cell. The analysis is also repeated by taking the lowest in tensity value for each land-use class. The points used to generate the point pattern are attached in Annex 1.

5.3   INTENSITY MAP FOR SPECKLE PATTERNS

To draw the intensity map of the the speckle pattern a gaussian kernel is used in the spatstat package. The bandwidth of the kernel affect the visual appearance of the map. Bandwidth size 10 is selected to draw the intensity map of the three land-use classes by comparing the visualization obtained from different bandwidth size.

5.4   DISTANCE FUNCTION ANALYSIS AND MONTE CARLO TEST

Based on the intensity map of the the different land-use class, stationary point pattern analysis is used. The homogeneous nearest-neighbor distances (F, G and J functions) and the Ripley's K functions are applied to check whether the speckle pattern is clustered or randomly distributed. For each distance function 39 simulation of CSR were simulated which means 95 percent envelopes are developed to test the deviation from the complete spatial randomness. 99 percent global envelopes are used to test the strength of clustering.

5.5   TESTING THE ANALYSIS PROCEDURE

The whole procedure of analysis has been tested on another radar image, ALOS PALSAR HH polarization image of Nairobi city. A park area which is almost free from strong reflectors is selected to test the analysis procedure. A sub set image of 100 by 100 pixel dimension has been taken.

Chapter 6

Results

This chapter shows the result obtained from the analysis of the spatial patterns of speckle for forest, agriculture and urban land-use classes.

6.1 FITTING THE GAMMA DISTRIBUTION

Speckle intensity has gamma distribution in multilook image. The equivalent number of looks(ENL) is used as a shape parameter to draw the gamma distribution. The ENL is used as a shape parameter by relating the the probability density function of the speckle intensity Equation 2.2 with the density for gamma distribution found in R package Equation 5.1. The number of looks obtained from the radar processor is 5. But this may not be the true equivalent number of looks of the radar because of spatial auto correlation that means neighboring pixels are not completely independent. By taking subset image from homogeneous area(Figure 6.1), ENL value of 3.6 is obtained using equation 2.3.
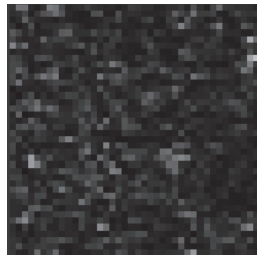
Figure 6.1: Subset homogeneous forest area SAR image
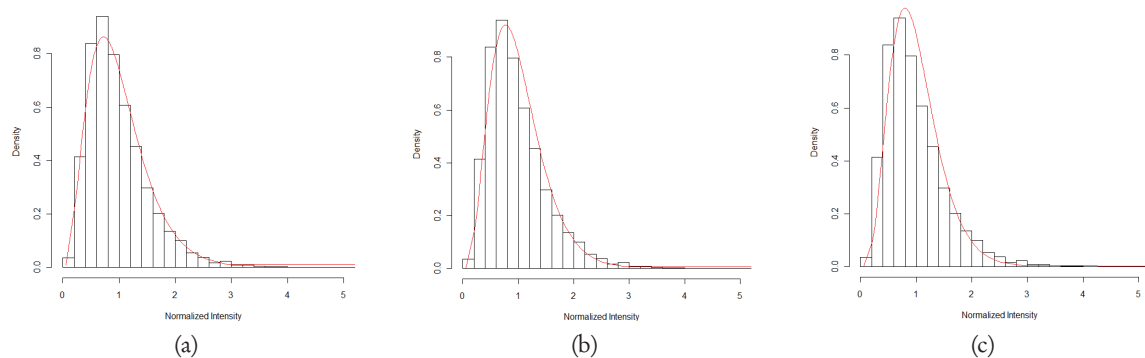
Figure 6.2: Gamma distribution of intensity in subset forest area; (a) using ENL 3.6; (b) using ENL 4.3; (c) using ENL 5

It is difficult to get truly homogeneous area from the image due to the heterogeneity the study area. So experiments are done using ENL value 3.6, 4.3 and 5 to select the best ENL value which fit the intensity histogram(Figure 6.2). ENL value of 4.3 is selected as shape parameter of the the gamma distribution to since better visualization is observed in this case and again the true ENL is expected between the value obtained by calculation which is 3.6 and the radar processor ENL which is 5. By using different ENL value different numbers of outliers are obtained which affect the spatial patterns of the speckles since the outliers are removed from the data to calculate the speckle pattern.

(a)   (b)
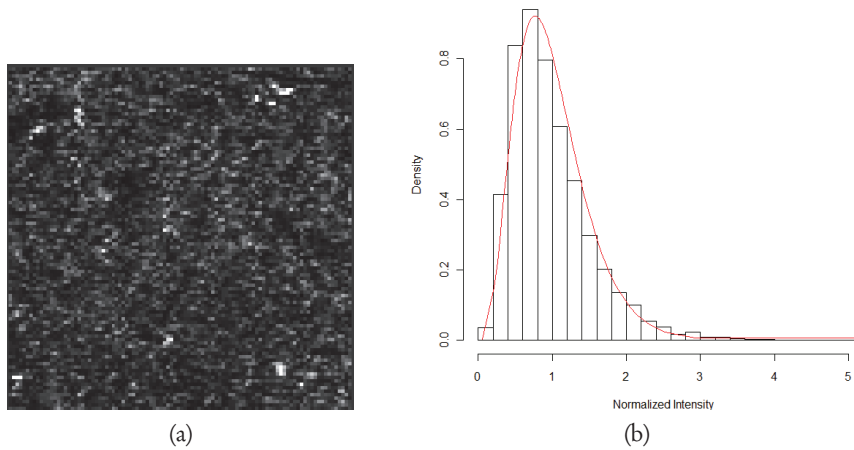
Figure 6.3: (a) Subset Forest area SAR image; (b) Histogram of the subset forest area.

(a)   (b)
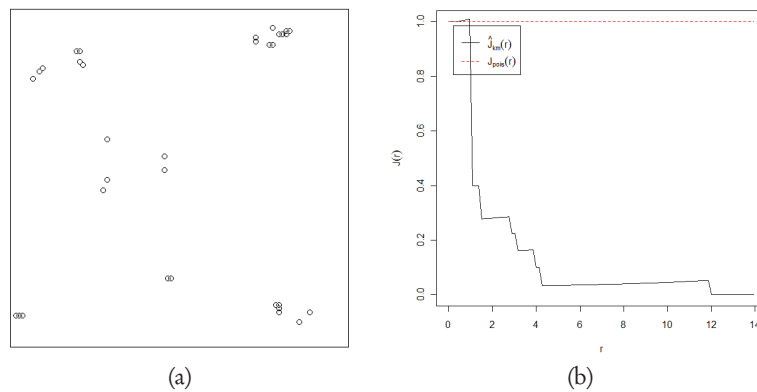
Figure 6.4: (a) Spatial point pattern of forest area strong reflectors; (b) J function of the pattern.

Land-use classes of forest, agriculture and urban which have 100 by 100 pixel dimensions are selected to study the spatial pattern of speckles in multilook C-band SAR image as shown in Figures 6.3, 6.5and 6.7. A better fit of the gamma distribution to the histogram of the data is seen in forest area. Due to the heterogeneity nature of agricultural and urban area, the gamma distribution doesn't fit properly to the histogram of the data.

The intensity of the radar image for each land-use class is normalized by dividing the intensity by the average intensity of each land-use class. Normalizing the intensity of each land-use class by the average intensity decreases the variation of the intensity with in the land-use classes, helps to properly fit the the distribution curve to the histogram of the intensity and to compare the result
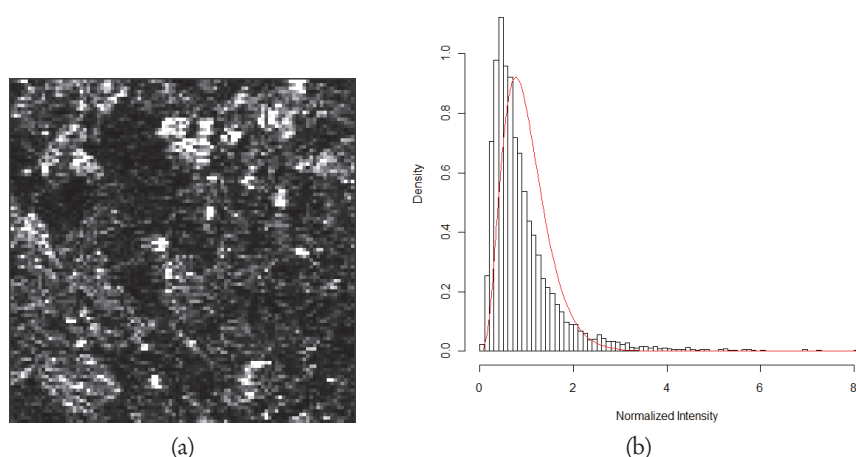
Figure 6.5: (a) Subset agricultural area SAR image; (b) Histogram of the subset agricultural area.
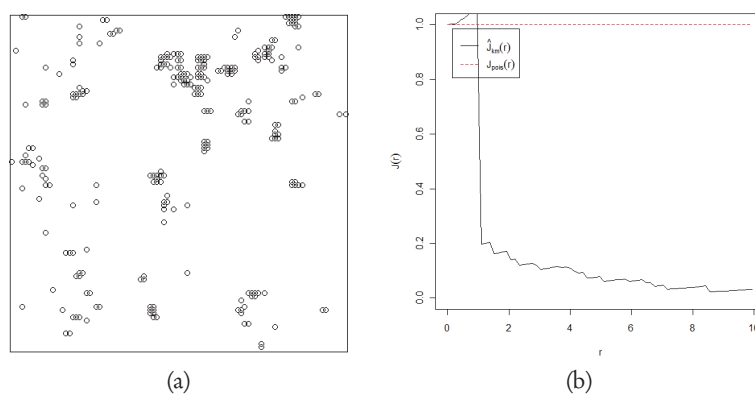
Figure 6.6: (a) Spatial point pattern of agricultural area strong reflectors; (b) J function of the pattern.

obtained from the different land-use classes.

By integrating the probability density function of the gamma distribution of speckle intensity, pixel intensity value which are unlikely to occur are identified. 33, 263 and 721 outliers are obtained in forest, agriculture and urban areas respectively. These outliers are the brightest pixels in the subset images. These outlier pixels cover building area in the image especially in urban and agricultural area and are considered as strong reflectors. The spatial point pattern of the strong reflectors are shown in Figures 6.4, 6.6 and 6.8. The spatial point pattern of the strong reflectors is clustered since the observed J function of the pattern is below the theoretical curve of poisson process. Most outliers are seen in urban area. The shape and arrangement of buildings create double bounce of the radar signal due to these urban area appear bright in the radar image. In the agricultural area also bright pixels are observed and 263 outliers are obtained from the analysis of the gamma distribution. The point pattern of these outliers matches the area covered by buildings.

The analysis clearly shows that all bright pixels appear in radar image are not due to speckle. Since speckle intensity has a gamma distribution, all pixels which are outliers due to the analysis of probability density functions are considered as strong reflectors.
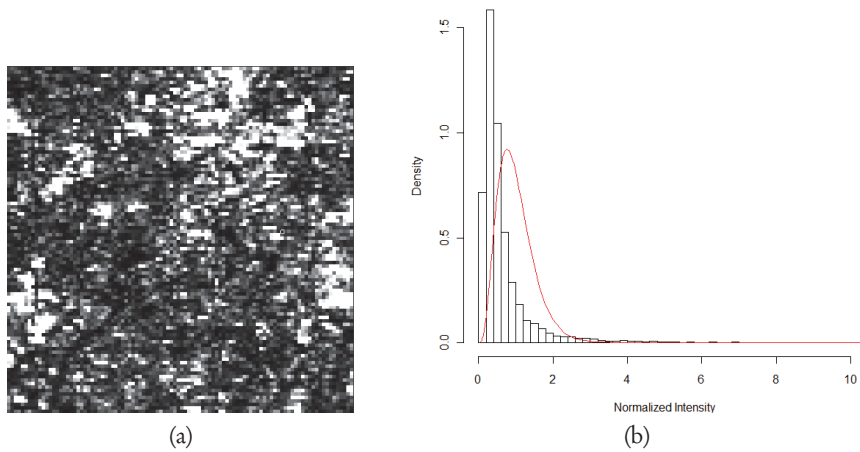
Figure 6.7: (a) Subset urban area SAR image; (b) Histogram of the subset urban area.
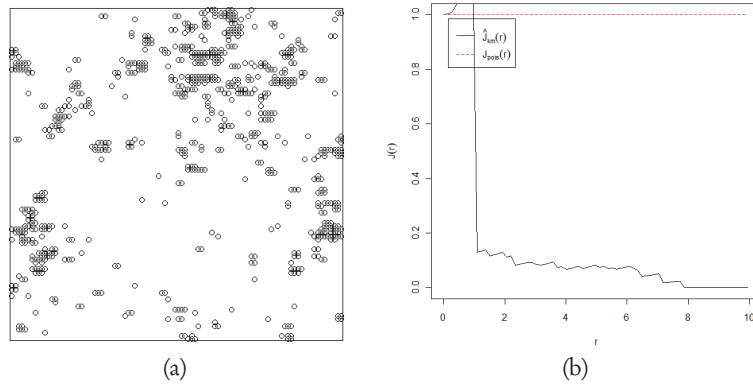
Figure 6.8: (a) Spatial point pattern of urban area strong reflectors; (b) J function of the pattern.

6.2   SPATIAL POINT PATTERN OF BRIGHT SPECKLES

To analyze the spatial patterns of bright pixels due to speckle, the corner reflectors are removed from the data.

Experiments are done to study the spatial pattern of speckle based on one percent and five percent assumption of the highest intensity value as speckled pixels. One percent of the highest intensity as speckled pixel is used to report in this section. The one percent speckled pixel is also included in the five percent assumption so that one percent of the highest intensity value can be a sample of bright speckles in the data. 100, 97 and 93 bright pixels are considered as speckled pixels in the forest, agriculture and urban land-use classes respectively. The spatial point pattern of the the bright speckles and the intensity map of the patterns are shown in Figure 6.9, 6.10 and 6.11. The intensity maps of the speckles show the variation of the density in local area. The intensity map of the speckles is drawn using gaussian kernel. Different bandwidth gives different visualization of the intensity. By comparing the result obtained from different bandwidths, bandwidth size 10 is selected to show the intensity map of the different land use class speckle patterns. The intensity maps of the speckle patterns of the land-use classes do not show non-stationarity process. So homogeneous distance functions are applied to further analyze the spatial point pattern of the speckles.

Figure 6.9: (a) Spatial point pattern of bright speckles in forest area; (b) Intensity map of the pattern.

Figure 6.10: (a) Spatial point pattern of bright speckles in agricultural area; (b) Intensity map of the pattern.

Figure 6.11: (a) Spatial point pattern of bright speckles in urban area; (b) Intensity map of the pattern.

6.3   POINTWISE MONTE CARLO TEST FOR BRIGHT SPECKLES

The deviation of the observed distance functions from CSR at a particular distance is tested by using pointwise Monte Carlo test. The observed distance functions for the forest area bright speckles and their associated 95 percent envelopes are shown in Figure 6.12 and 6.13. The x-axis shows the interaction distance in pixel dimension. One pixel dimension represents 20m on the ground. The observed F function graph for the speckles in the forest area shows clustered patterns at interaction distance greater than 5.5 pixel size(80 m). The observed G function graph displays clustered pattern between the range of interaction distance 20m to 90m. The observed J function plot displays clustered pattern between the range of interaction distance 20m to 170mand the maximum interaction is observed at 180m interaction distance. The observed K function graph shows a clustered pattern between the range of interaction distance 20m and 320m.

Figure 6.12: Envelopes for bright speckles in forest area: (a) F function; (b) G function.

Figure 6.13: Envelopes for bright speckles in forest area: (a) J function; (b) K function.

The observed distance functions for bright speckles in agricultural area and their associated 95 percent envelopes are shown in Figure 6.14 and 6.15. The observed K functions plots for speckles

in agricultural area displays significantly clustered pattern in any of the interaction distances. The observed F function plot shows significantly clustered pattern at interaction distance greater than 80m. The Observed G and J functions plots for speckles in agricultural area display significantly clustered pattern at interaction distance 20m to 170m and 20m to 200m respectively.

Figure 6.14: Envelopes for bright speckles in agricultural area: (a) F function; (b) G function.
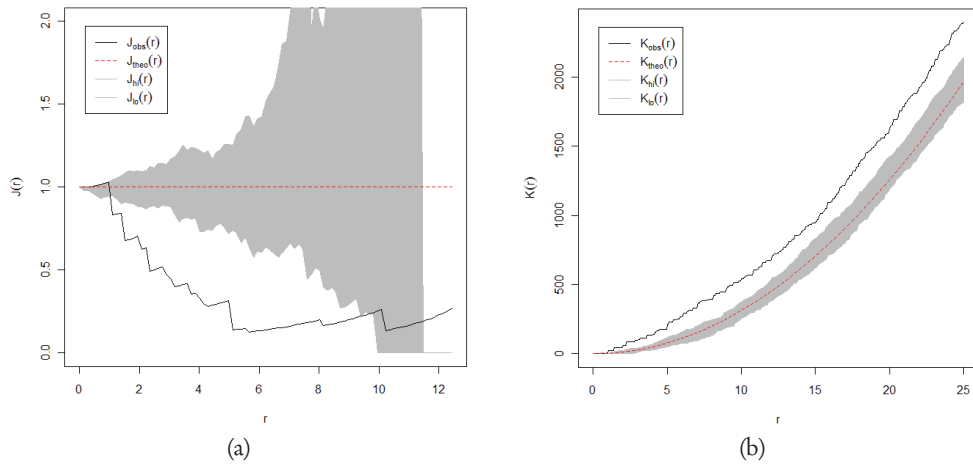
Figure 6.15: Envelopes for bright speckles in agricultural area: (a) J function; (b) K function.

The observed distance functions for speckles in urban area for the 39 simulation of CSR is given in Figure 6.16 and 6.17. The observed F function graph shows a CSR at all interaction distances. The observed G and J functions plots show a tendency for clustered pattern between interaction distances 20m to 100m . The K function graph shows a tendency of clustered pattern at interaction distance greater than 100m.

Figure 6.16: Envelopes for bright speckles in urban area: (a) F function; (b) G function.
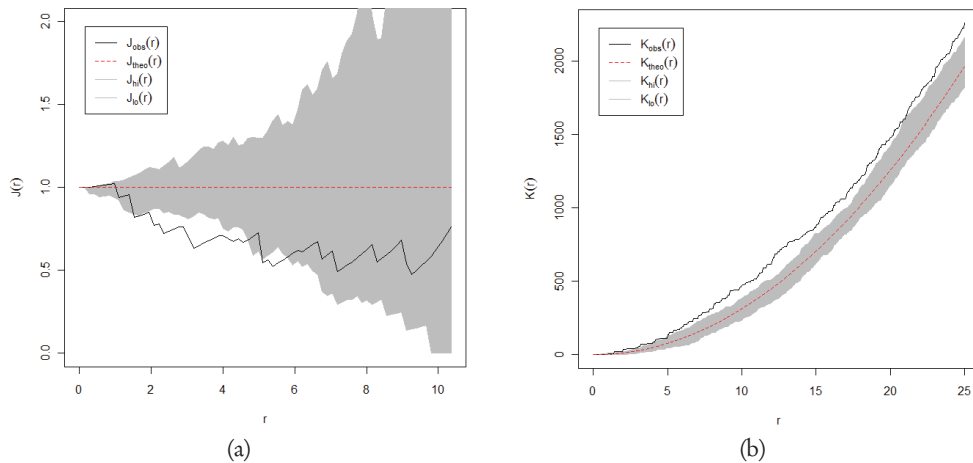
Figure 6.17: Envelopes for bright speckles in urban area: (a) J function; (b) K function.

6.4 SIMULTANEOUS MONTE CARLO TEST FOR BRIGHT SPECKLES

The simultaneous monte carlo test is used to test whether the observed distance functions are strongly or weakly deviate from the CSR of the different simulation of the CSR. The 19 simulation of the CSR is used to check the deviation of the the observed distance functions from the CSR. A weakly, moderately and strongly clustered pattern is observed for urban, forest and agricultural speckles respectively as shown in figure 6.18, 6.19 and 6.20 in the 19 simulation of CSR for each distance function in each land-use classes.
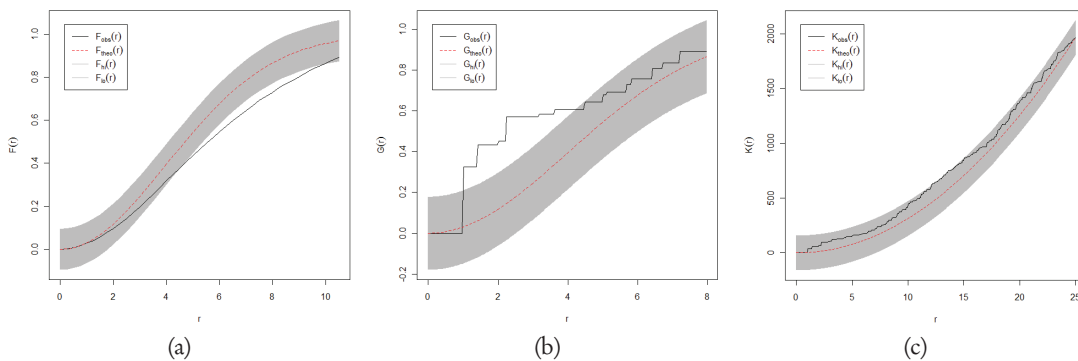
Figure 6.18: Global envelopes and observed distance functions for bright speckles in forest area: (a) F function; (b) G function; (c) K function.

Figure 6.19: Global envelopes and observed distance functions for bright speckles in agricultural area: (a) F function; (b) G function; (c) K function.
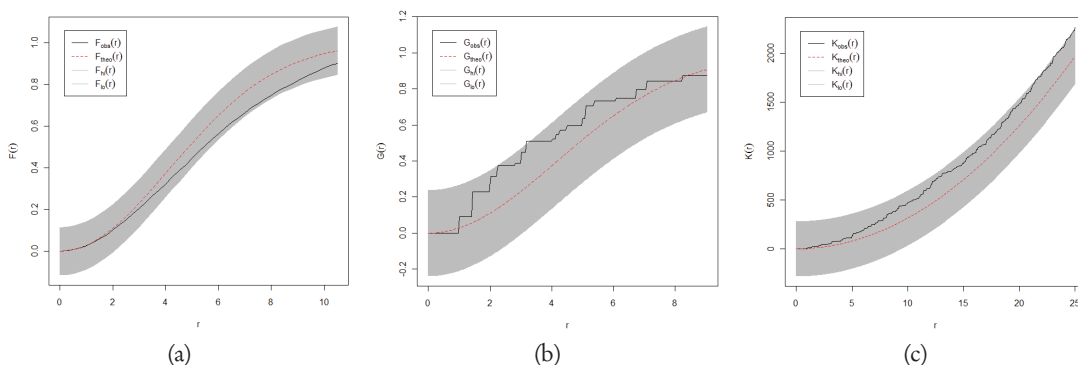
Figure 6.20: Global envelopes and observed distance functions for bright speckles in urban area: (a) F function; (b) G function; (c) K function.

6.5 SPATIAL POINT PATTERN OF DARK SPECKLES

The spatial pattern of bright and dark speckles should be studied separately since bright pixels are created due to constructive interference and dark speckles are created due to destructive interference of return signals from scatterers with in one resolution cell. The spatial pattern of dark speckles is analyzed by taking one percent of the lowest intensity value in each land use-class. The spatial pattern of the dark speckles for the land use-classes forest, agriculture and urban area are shown in Figures 6.21, 6.22 and 6.23 respectively. 100, 97 and 93 points are taken as speckled pixels based on the analysis of one percent of the lowest intensity value for forest, agriculture and urban land-use classes respectively.

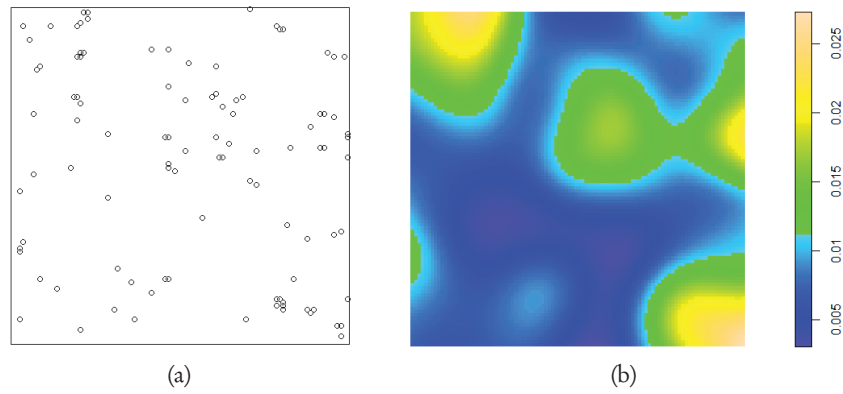(a)   (b)
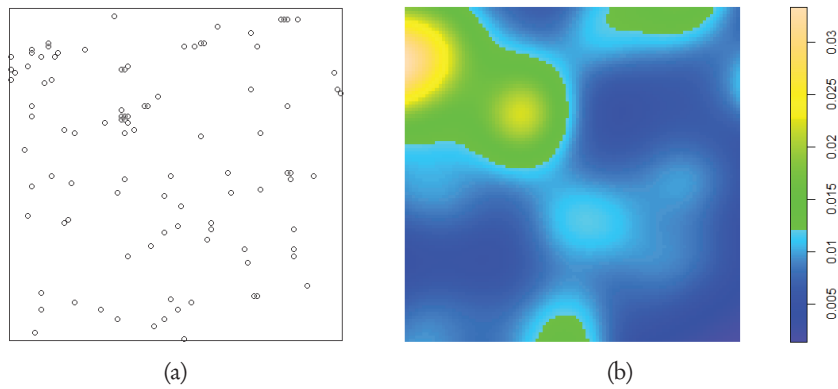
Figure 6.21: (a) Spatial point pattern of dark speckles in forest area; (b) Intensity map of the pattern.
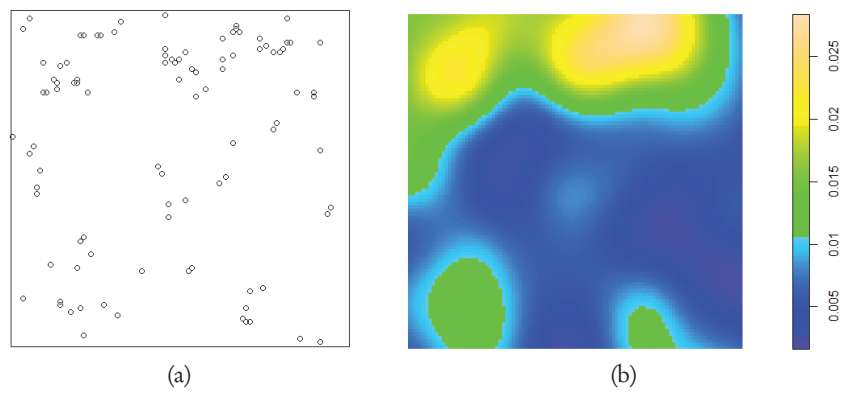

(a)   (b)
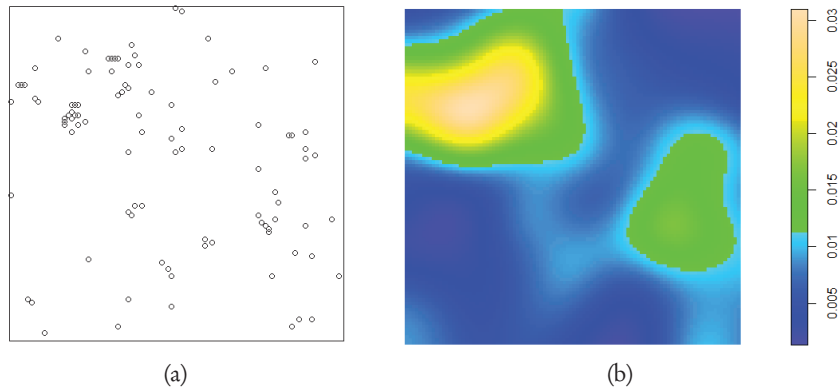
Figure 6.22: (a) Spatial point pattern of dark speckles in agricultural area; (b) Intensity map of the pattern.
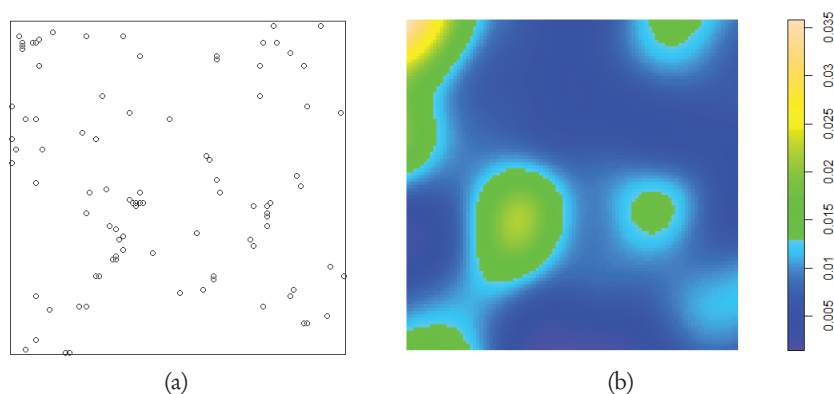
Figure 6.23: (a) Spatial point pattern of dark speckles in urban area; (b) Intensity map of the pattern.

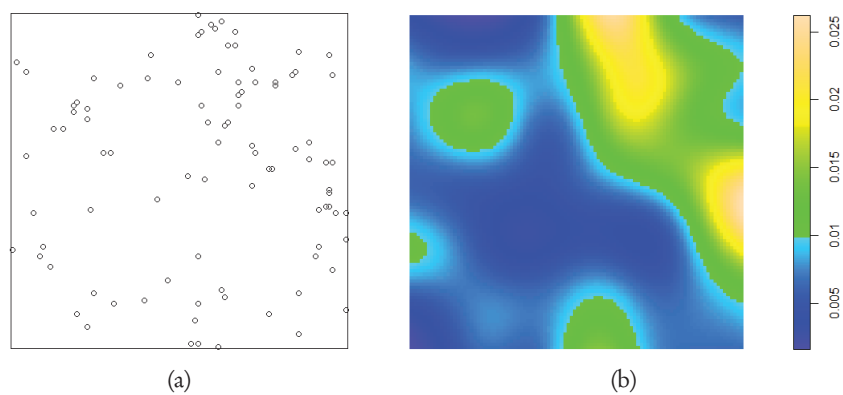## 6.6 MONTE CARLO TEST FOR DARK SPECKLE PATTERN

The observed distance functions for the forest area dark speckles and their associated 95 percent envelopes are shown in Figure 6.24 and 6.25. The observed F function plot shows CSR for all interaction distances. The observed G function shows a tendency of clustered pattern in the range of interaction distance 20m to 100m. The observed J functions shows a tendency of clustered pattern in the range of interaction distance 20m to 140m. The observed K function also shows a tendency of clustered pattern in the range of interaction distance 20m to 300m.

The observed distance functions for the agricultural area dark speckles and their associated 95 percent envelopes are shown in Figure 6.26 and 6.27. The observed F function plot shows a significantly clustered pattern in the range of interaction distance greater than 60m. The observed G and J functions plots show a significantly clustered pattern in the range of interaction distance 20m to 120m. The observed K function shows a significantly clustered pattern in all interaction distances.
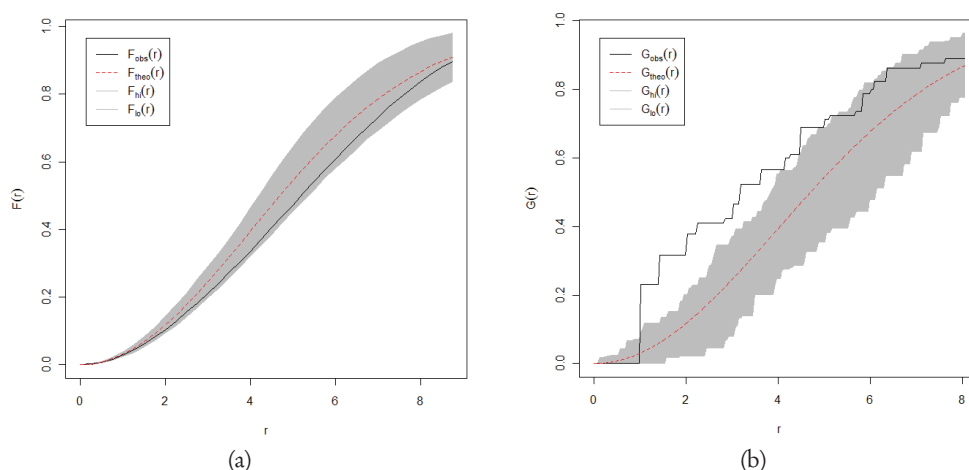
Figure 6.24: Envelopes for dark speckles in forest area: (a) F function; (b) G function.

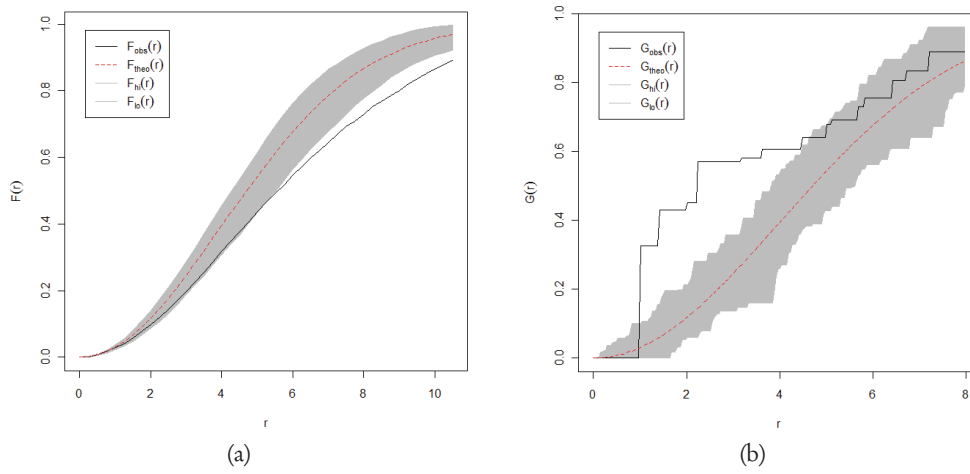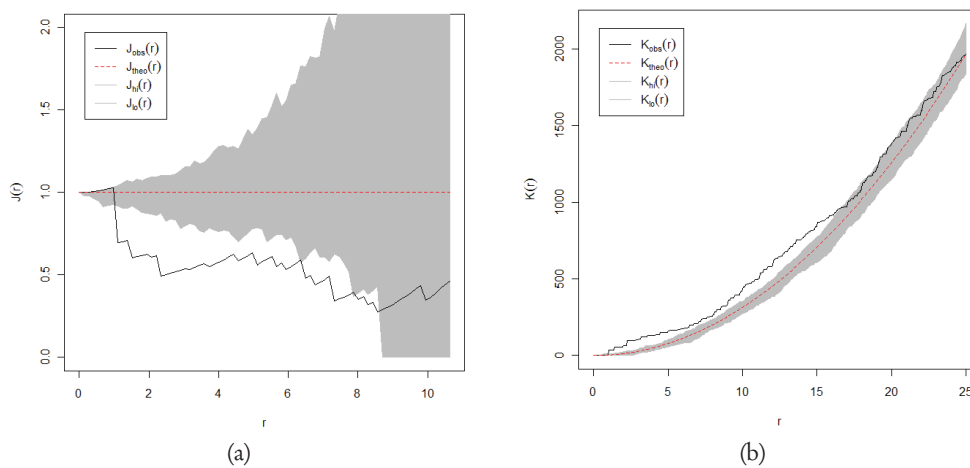The observed distance functions for the urban area dark speckles and their associated 95 per-
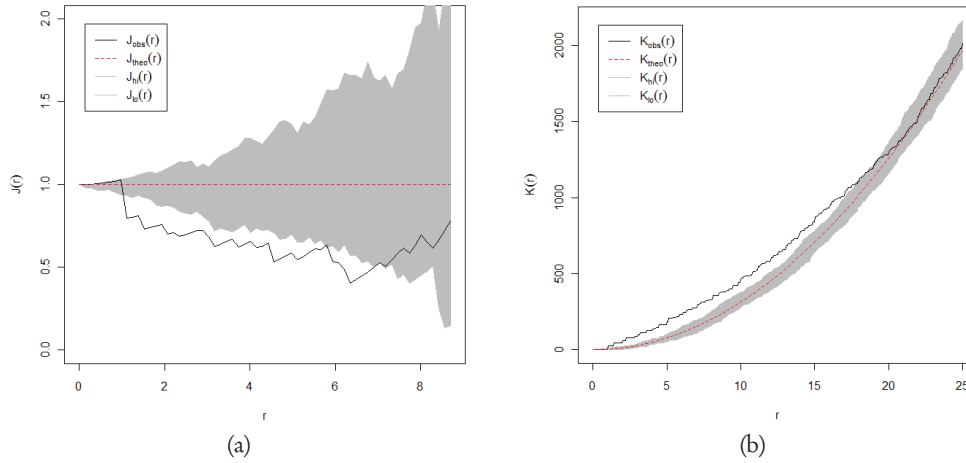
Figure 6.25: Envelopes for dark speckles in forest area: (a) J function; (b) K function.
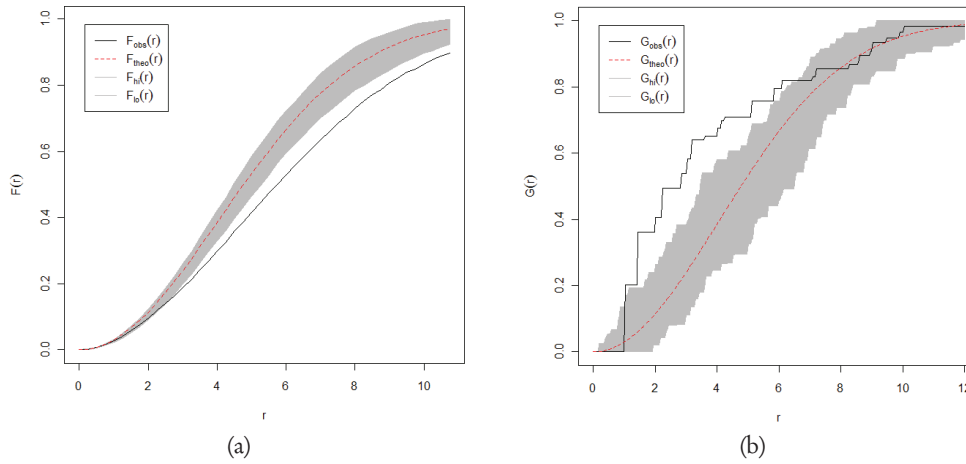
Figure 6.26: Envelopes for dark speckles in agricultural area: (a) F function; (b) G function.

cent envelopes are shown in Figure 6.28 and 6.29. The observed F function plot shows a tendency of clustered pattern in the range of interaction distance 80m to 160m. The observed G function graph shows a clustered pattern in the range of interaction distance 20m to 100m. The observed J function graph also shows a clustered pattern in the range of interaction distance 20m to140m. The observed K function shows a clustered pattern in the range of interaction distance 20m to 360m.
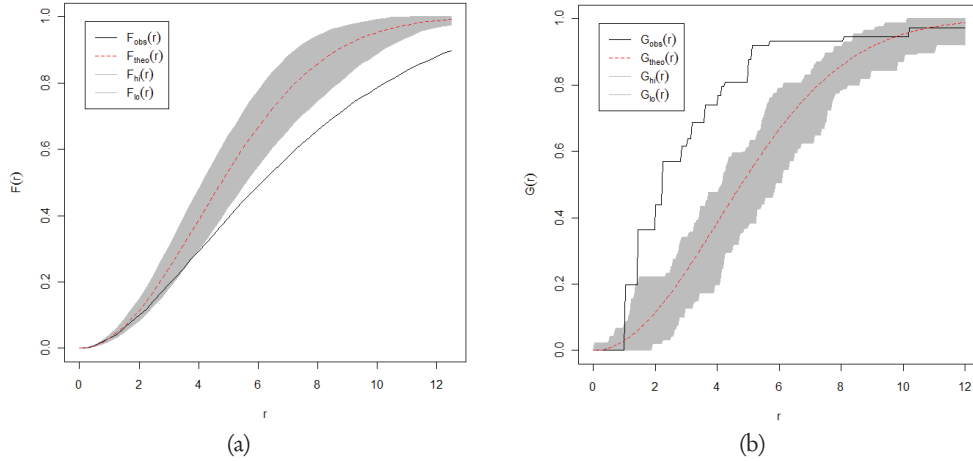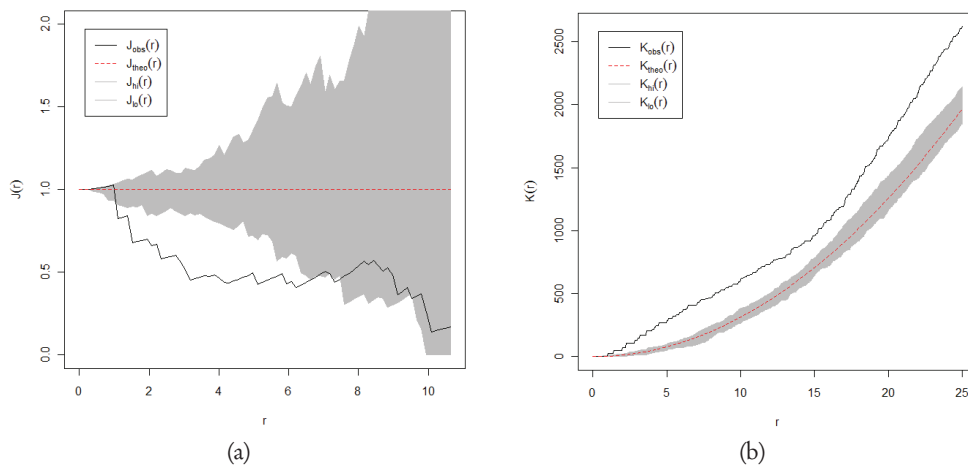
Figure 6.27: Envelopes for dark speckles in agricultural area: (a) J function; (b) K function.
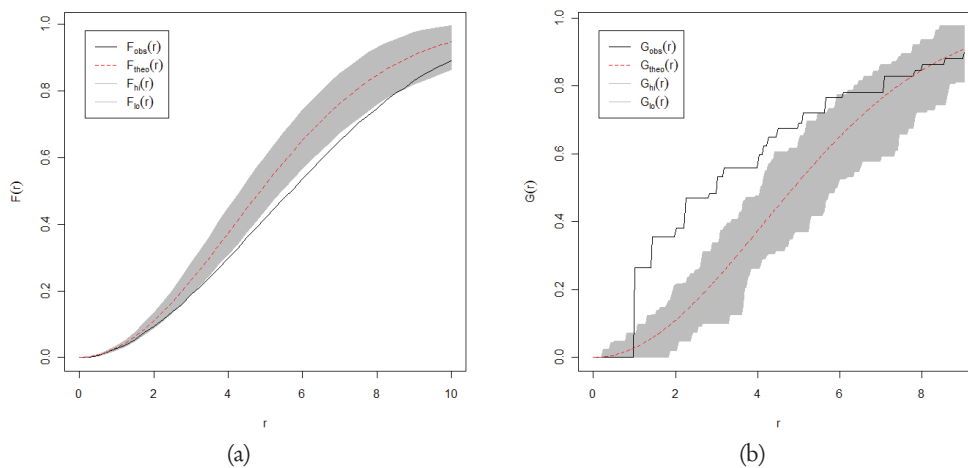
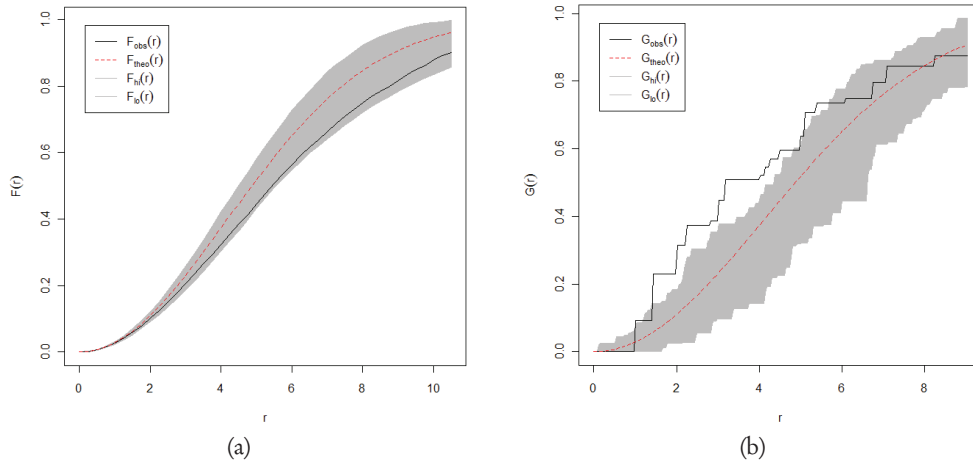Figure 6.28: Envelopes for dark speckles in urban area: (a) F function; (b) G function.
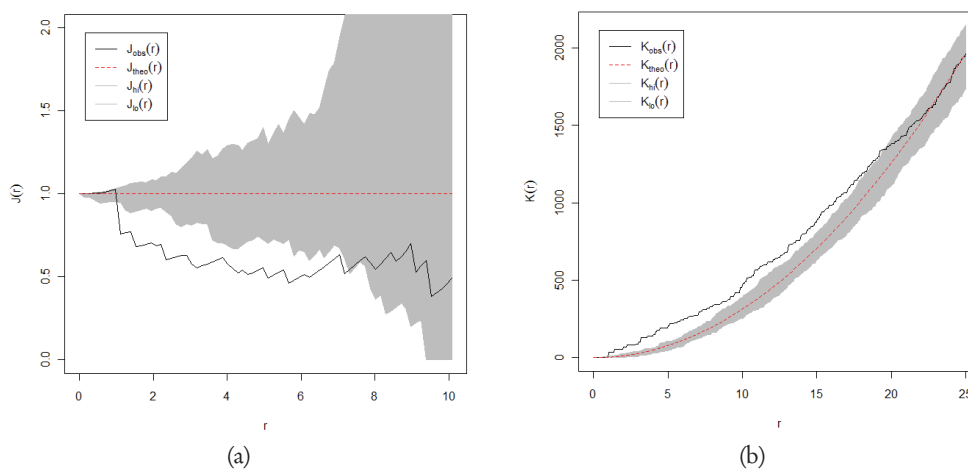
Figure 6.29: Envelopes for dark speckles in urban area: (a) J function; (b) K function.

6.7 SIMULTANEOUS MONTE CARLO TEST FOR DARK SPECKLES

The simultaneous monte carlo test is used to test whether the observed distance functions are strongly or weakly deviate from the CSR of the different simulation of the CSR. The 19 simulation of the CSR is used to check the deviation of the the observed distance functions from the CSR. A weakly clusterd pattern is observed for forest and urban area dark speckles as shown in Figure 6.30 and 6.32 respectively . A moderate clustered pattern is observed for agricultural area dark speckles as shown in Figure 6.31.
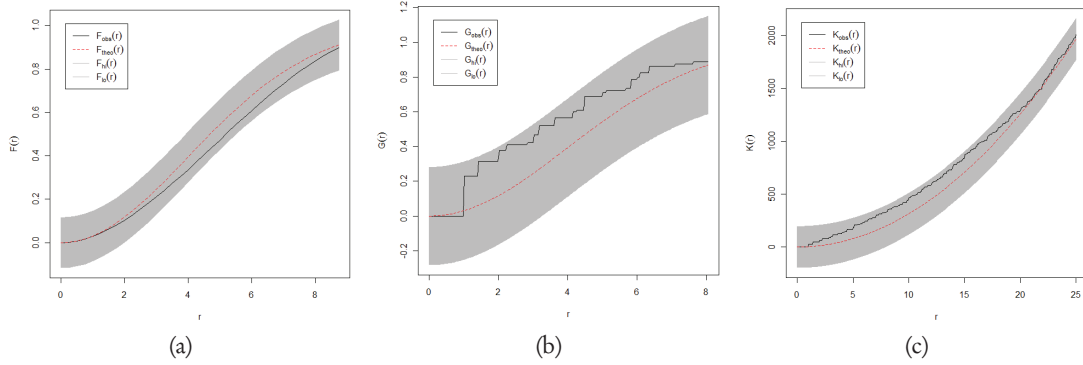
Figure 6.30: Global envelopes and observed distance functions for dark speckles in forest area: (a) F function; (b) G function; (c) K function.
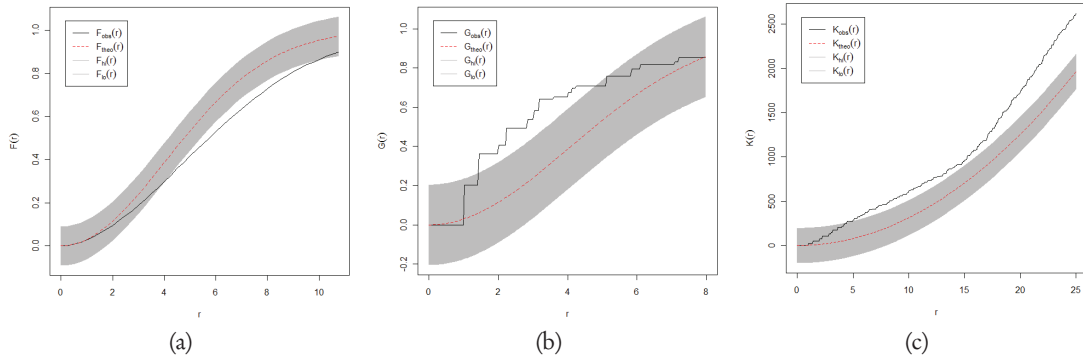
Figure 6.31: Global envelopes and observed distance functions for dark speckles in agricultural area: (a) F function; (b) G function; (c) K function.
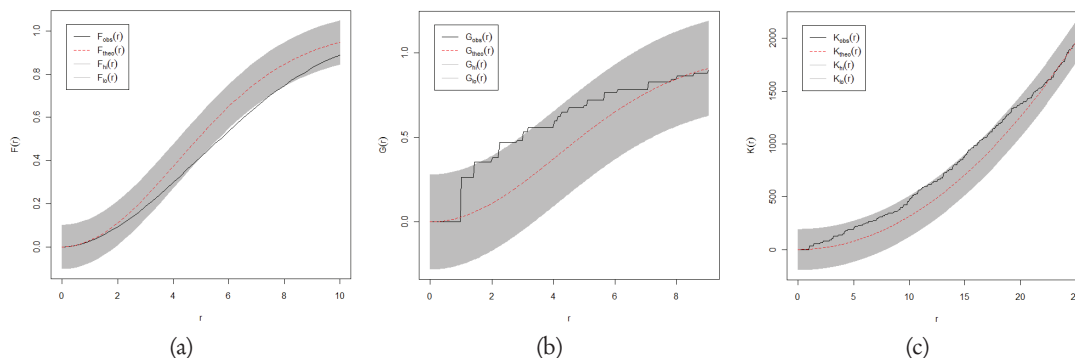
Figure 6.32: Global envelopes and observed distance functions for dark speckles in urban area: (a) F function; (b) G function; (c) K function.

6.8   SPECKLE IN AGRICULTURAL AREA OBJECTS

Another way to study the speckle pattern is by combining neighborhood speckled pixel together and analyzing the pattern. Bright agricultural speckles are taken to analyze patches of speckles. The spatial pattern of 59 points of speckled agricultural features is shown in Figure 6.33. The intensity map shows the variation in the density of speckles in the subset image. The pointwise Monte Carlo test shows a CSR in all interaction distances in the 95 percent envelope as shown in Figure 6.34 and 6.35. The 90 percent global envelope also shows a CSR of the speckled features in agricultural area as shown in Figure 6.36.
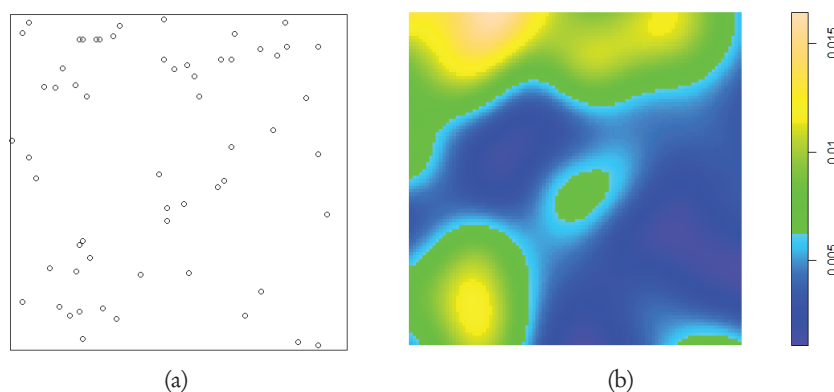
Figure 6.33: (a) Spatial point pattern of speckled objects in agricultural area; (b) Intensity map of the pattern.
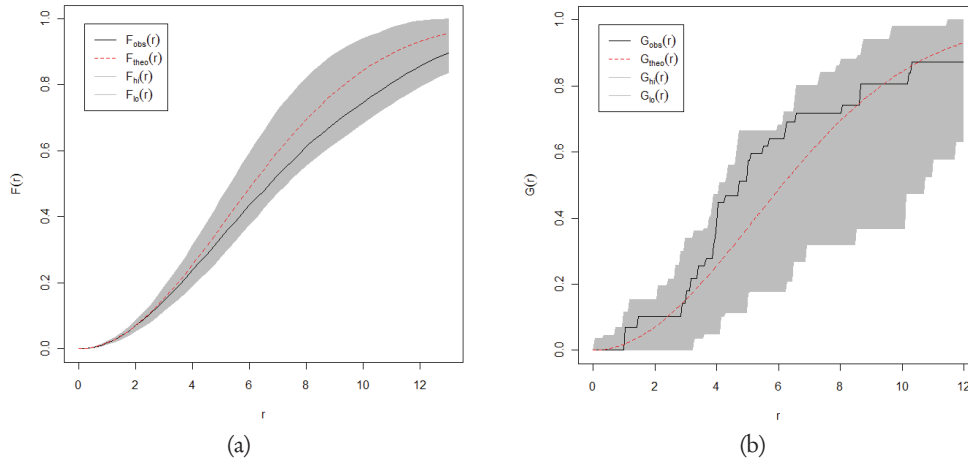
Figure 6.34: Envelopes for speckled objects in agricultural area: (a) F function; (b) G function.
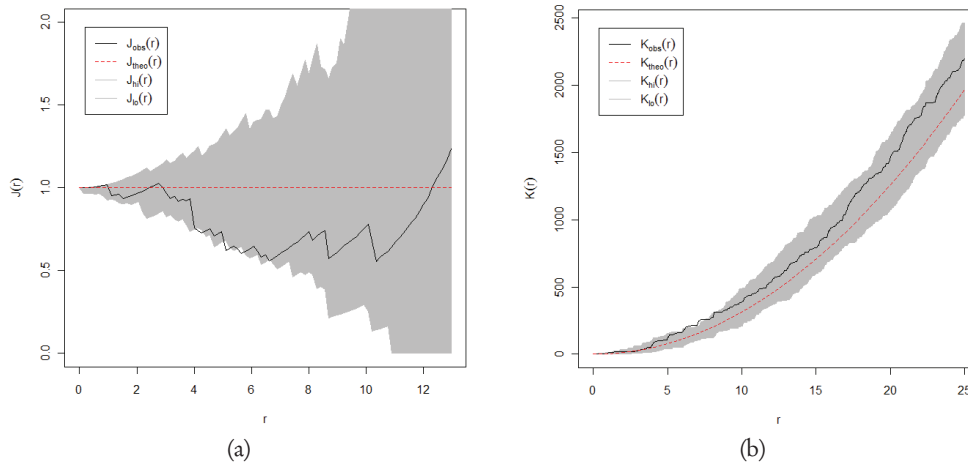
Figure 6.35: Envelopes for speckled objects in agricultural area: (a) J function; (b) K function.
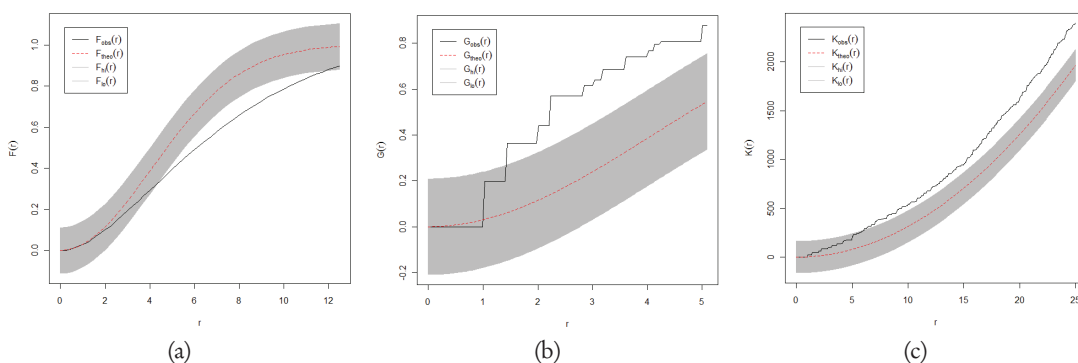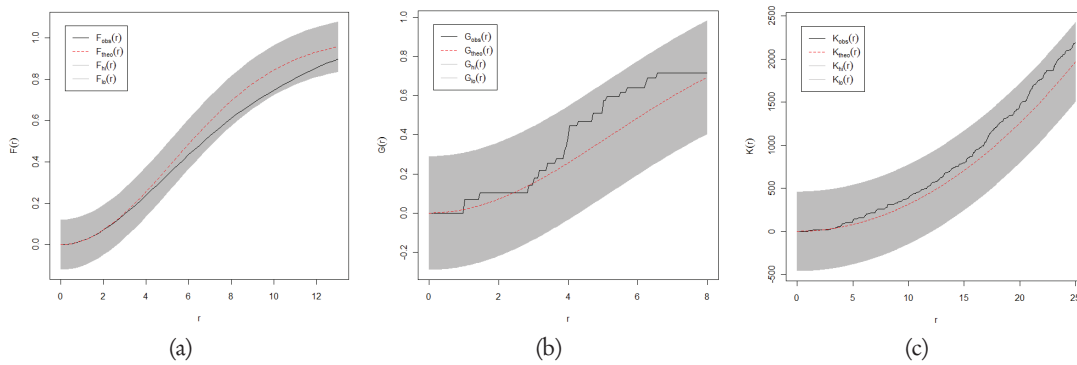

Figure 6.36: Global envelopes and observed distance functions for speckled objects in agricultural area: (a) F function; (b) G function; (c) K function.

6.9   SPECKLE IN PARK AREA NAIROBI CITY

The analysis procedure is tested by taking park area from Nairobi city SAR image. The park area is almost homogeneous area which is free of strong reflectors. The ENL obtained from the radar processor is 2. But this value should be checked by taking homogeneous area from the image. The subset image is already homogeneous(Figure 6.37) and taking the ratio of mean of the subset image to the standard deviation ENL value of 1.8 is obtained. Shape parameter 1.8 is used to draw the gamma distribution. The gamma distribution fit the histogram properly as shown in Figure 6.37. By integrating the gamma distribution 5 outliers are obtained from10000 pixels of the subset image. After removing the outliers one percent of the highest intensity is assumed as speckled pixel. 100 pixels are considered as bright speckles and the spatial pattern is shown in Figure 6.38. The intensity map of the bright speckles doesn't show non- stationarity point process so homogeneous distance functions are used to analyze the speckle pattern. A clustered pattern of bright speckles is observed in the park area by comparing the observed distance functions to the theoretical Poisson distribution as shown in Figures 6.39 and 6.40.

(a)   (b)
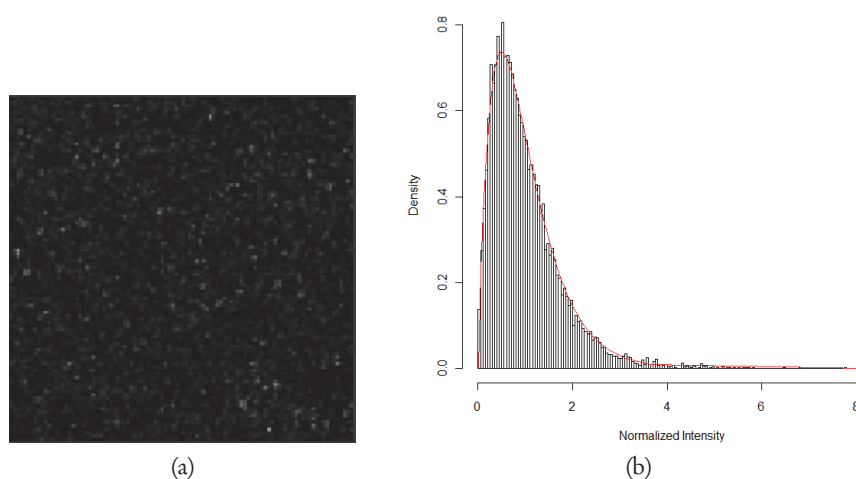
Figure 6.37: (a) Subset park area SAR image; (b) Histogram of the subset park area.

(a)   (b)
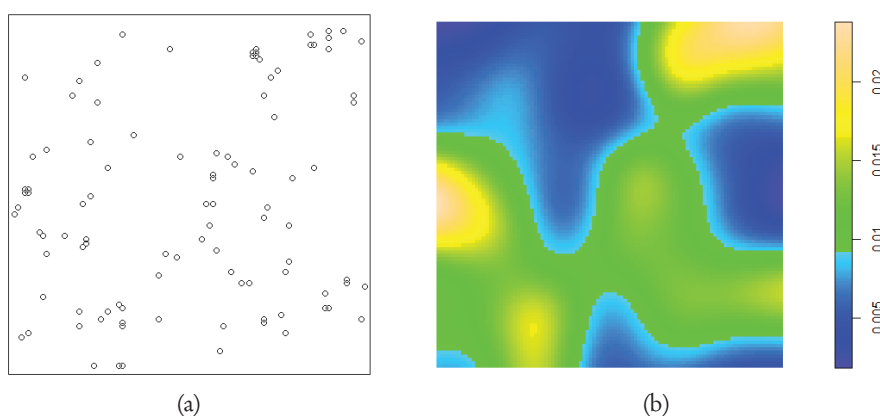
Figure 6.38: (a) Spatial point pattern of bright speckles in park area; (b) Intensity map of the pattern.
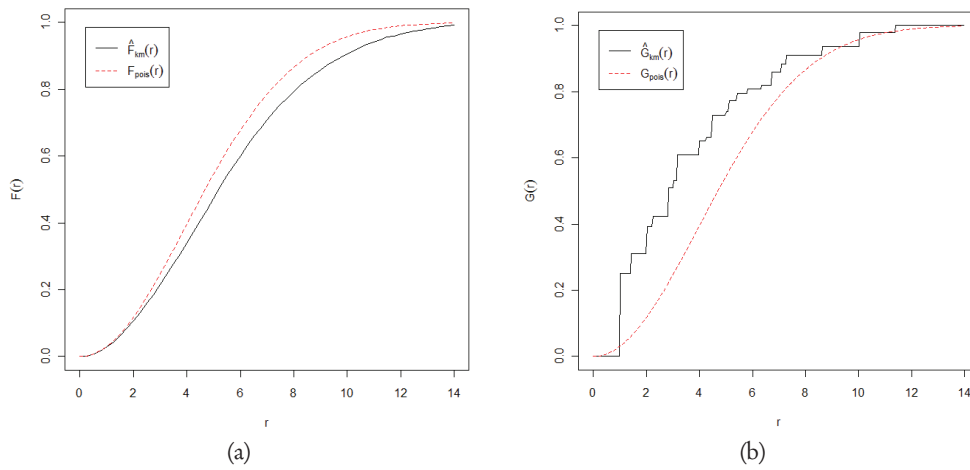
Figure 6.39: Distance functions for bright speckles in park area: (a) F function; (b) G function.
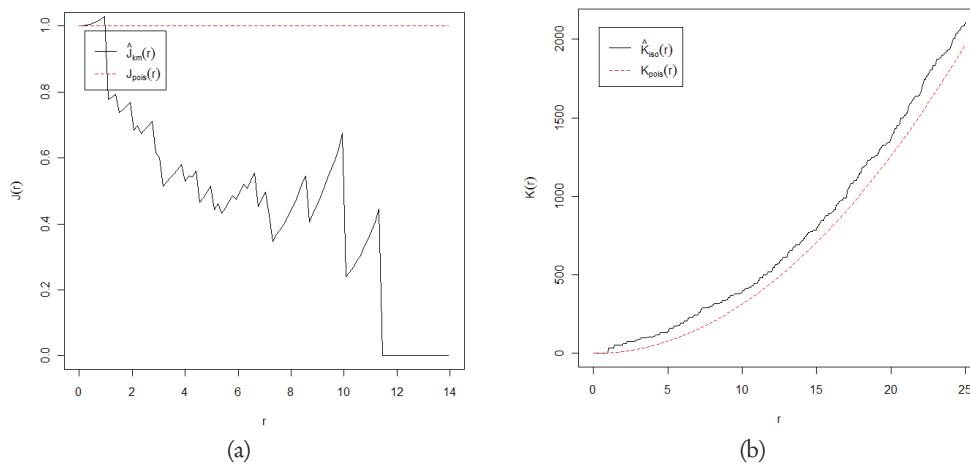
Figure 6.40: Distance functions for bright speckles in park area: (a) J function; (b) K function.

Chapter 7

Discussion

The aim of the study is to characterize the spatial pattern of speckle using nearest-neighbor distance functions and Ripley's K function. Spatial pattern of bright speckles and dark speckles of forest, agriculture and urban land-use classes are studied.

Not all bright pixels in the image are due to speckle therefore in this study strong reflectors are removed from the data. Gamma distribution of intensity is applied to differentiate strong reflectors from speckle. The ENL is used as shape parameter of the gamma distribution. The number of looks obtained from the radar processor is 5. But this may not be the true equivalent number of looks of the radar because of spatial auto correlation that means neighboring pixels are not completely independent.

The ENL is estimated by taking homogeneous area from the image. It is difficult to get a truly homogenous area due to the heterogeneity of the land-use classes in the study area. ENL value of 4.3 is selected as shape parameter of the gamma distribution since better visualization is observed in this case and again the true ENL is expected between the value obtained by calculation which is 3.6 and the radar processor ENL which is 5. By using different ENL value different numbers of outliers are obtained which affect the spatial patterns of the speckles since the outliers are separated from the data to calculate the speckle pattern.

Integrating the probability density function of the gamma distributions, pixels which are unlikely to occur above a certain intensity value are considered as outliers. By analyzing the spatial pattern of the outliers, the outliers are the brightest pixels in the image. Most of the outliers form blocks of bright pixels which correspond to the arrangement of buildings in the study area and are considered as corner reflectors in the study area. The analysis is also tested by taking park area from Nairobi city SAR image. The park area is almost free of strong reflectors. Through the analysis of gamma distribution only 5 pixels are considered as outliers from 10000 pixels of the subset park area image.

The application of gamma distribution of intensity helps to differentiate between speckle and strong reflectors. The analysis has shown that most of the brightest pixels in the study area are due to strong reflectors rather than speckles. This has contribution in the understanding of SAR image. It helps to clarify that salt and pepper appearance of SAR image is not only due to speckle but also due to strong reflectors.

After strong reflectors are removed from the data, one percent of the highest intensity value is used as speckled pixels to analyze the spatial pattern of bright speckles in each land-use class. The spatial patterns of the dark speckles are also analyzed by taking one percent of the lowest intensity value for each land-use class. Different assumptions of threshold value for speckled pixels change the interaction distance of the speckles even if clustered pattern is observed in the one percent and five percent assumption of thresholds. So the interaction distance for speckle is therefore sensitive to both the change in the ENL and threshold assumption even if clustered pattern is obtained from the different assumption experiments.

From the analysis of distance functions of bright and dark speckles, the observed G and J functions clearly show the nearest neighbour interaction between speckle pattern. A significantly

clustered pattern of speckle is observed in the subset agricultural area SAR image. Agricultural fields are prepared and planted in a very orderly fashion. The row orientation may play an important role in radar return from agricultural fields which may create the constructive interference of the return signal within one resolution cell. If penetration through vegetation cover occurs the underline soil may also contribute to the radar return. The moisture content of the soil may also influence the dielectric property of the soil which has influence in scattering of the incident signal in the agriculture area.

The Monte Carlo test for 19 simulation of the CSR displays a moderately clustered pattern for the speckles in urban area. In urban area most of the features are arranged in systematic pattern. The features form blocks which may have significance influence in the interference of return radar signals within one resolution cell.In forest area a moderately clustered pattern of speckles is observed. This may be the trees in the forest area are not oriented in row orientation like in agriculture area.

The analysis of bright speckled agricultural objects shows that the spatial pattern of the speckled agricultural objects is random pattern for both 95 percent pointwise envelopes and 99 percent global envelopes as shown in Figure 6.36. This shows that considering patches of speckle in the spatial pattern analysis gives a different result.

The analysis carried in park area Nairobi city also shows a clustered pattern of speckle especially in the observed J function. The analysis generally shows that analyzing radar speckle using spatial point pattern analysis gives promising result in the understanding of radar speckle which has great input in SAR image analysis.

Chapter 8

Conclusion and Recommendation

The main objective of the study is the spatial patterns of speckle in SAR image. The analysis followed to distinguish bright speckles from srong reflectors using integration of gamma distribution of the intensity gives promising result. Based on this analysis pixels which are unlikely to occur are considered as strong reflectors and are separated from the data to analyze the speckle pattern. Then one percent of the highest and also one percent of the lowest intensity pixel value is taken to analyze the speckle pattern even if the exact number of speckle pattern is not know. Strong clustering of speckles is observed in the agricultural area from the analysis of bright and also dark speckles. Moderate clustering of speckles is observed in urban and forest area. Considering speckled objects rather than speckled pixels in agricultural area, the spatial pattern of speckles has changed to CSR.

The whole analysis procedure is tested by taking HH Polarization ALOS PALSAR image by taking park area from Nairobi city. The area is almost free of strong reflectors and a clustered pattern of speckles is obtained from the analysis. From these results we can conclude that spatial point pattern is powerful to analyze the speckle spatial pattern and also shows the relationship between land cover type and speckle pattern. It is also possible to conclude that the brightest pixels in SAR image especially in urban area is due to strong reflectors rather than speckles.

Further study is recommended in agriculture area by considering different level of plant growth. The stage of the plant growth may affect the radar reflectivity and also the kind of vegetation plotted on the field during imaging may also affect the spatial pattern of speckles.

Bibliography

[1] S. Anwar. Implementation of strauss point process model to earthquake data. Master's thesis, University of Twente, 2009.

[2] A. Baddeley. Analysing spatial point patterns in R. Technical report, 2008.

[3] A. Baddeley and R. Turner. spatstat: An R package for analyzing spatial point patterns. *Jornal of statistical software*, 12(6):1–42, 2005.

[4] A. J. Baddeley, J. Moller, and R. Waagepetersen. Non- and semi-parametric estimation of interaction in inhomogeneous point patterns. *Statistica Neerlandica*, 54(3):329–350, 2000.

[5] S. Chitroub, A. Houacine, and B. Sansal. Statistical characterisation and modelling of SAR images. *Signal Processing*, 82(1):69–92, 2002.

[6] J.S. Daba and P. Jreije. Advanced stochastic models for partially developed speckle. *World Academy of Science, Engineering and Technology*, 41:566–570, 2008.

[7] P. Diggle. *Statistical analysis of spatial point patterns*. Arnold, London, 2nd edition, 1983.

[8] V. Frost, J. Stiles, K. Shanmugan, and J. Holtzman. A model for radar images and its application to adaptive digital filtering of multiplicative noise. *IEEE Transactions on pattern analysis and machine intelligence*, 4(2):157–166, 1982.

[9] L. Gagnon and A. Jouan. Speckle filtering of SAR images - A comparative study between complex-wavelet-based and standard filters. In *Wavelet applications in signal and image processing*, volume 3169, pages 80–91, 1997.

[10] A. Gatrell, T. Bailey, P. Diggle, and B. Rowlingson. Spatial point pattern analysis and its application in geographical epidemiology. *Transactions of the Institute of British Geographers*, 21(1):256–274, 1996.

[11] A. Gelfand, P. Diggle, M. Fuentes, and P. Guttorp. *Handbook of spatial statistics*. CRC, 2010.

[12] D. Gleich and M. Datcu. Wavelet-based despeckling of SAR images using Gauss-Markov random fields. *IEEE Transactions on geoscience and remote sensing*, 45(12, Part 2):4127–4143, 2007.

[13] J. W. Goodman. Some fundemental properties of speckle. *Journal of the Optical Society of America*, 66(11):1145–1150, 1976.

[14] K. K. Gupta and R. Gupta. Feature preserving speckle filtering of the SAR images by wavelet transform. *Photonirvachak-Journal of the Indian Society of Remote Sensing*, 36(1):51–60, 2008.

[15] R.F. Hanssen. *Radar Interferometry - Data Interpretation and Error Analysis*. Springer, Dordrecht, 1st edition, 2001.

[16] D. Kuan, A. Sawchuk, T. Strand, and P. Chavel. Adaptive restoration of images with speckles. *IEEE Transactions on acoustics speech and signal processing*, 35(3):373–383, 1987.

[17] R. S. Lu. Geometrical information extraction from laser speckle pattern images using texture analysis. In *Third International Symposium on Precision Mechanical Measurements, Pts 1 and 2*, volume 6280, pages U457–U462, 2006.

[18] R. Marques, E. Carvalho, R. Costa, and F. Medeiros. Filtering effects on SAR images segmentation. In *Telecommunications and Networking - ICT*, volume 3124, pages 1041–1046. Springer Berlin / Heidelberg, 2004.

[19] M. Nicklawy, A. F. Hassan, M. Ballrawi, N. Farid, and A. M. Sanjid. Characterizing surface roughness by speckle pattern analysis. *Journal of Scientific & Industrial Research*, 68(2):118–121, 2009.

[20] C. Oliver and S. Quegan. *Understanding synthetic aperture radar images*. Artech House, Boston, 1998.

[21] K. Ouchi. Statistics of speckle in synthetic aperture radar imagery from targets in random motion. *Optical and Quantum Electronics*, 13(2):165–173, 1981.

[22] G. L. W. Perry, B. P. Miller, and N. J. Enright. A comparison of methods for the statistical analysis of spatial point patterns in plant ecology. *Plant Ecology*, 187(1):59–82, 2006.

[23] J.A. Richards. *Remote sensing with imaging radar*. Springer, Heidelberg, 2009.

[24] Y. Sheng and Z. Xia. A comprehensive evaluation of filters for radar speckle suppression. In *International Geoscience and Remote Sensing Symposium (IGARSS 96): Remote Sensing for a Sustainable Future*, pages 1559 –1561, 1996.

[25] A. Stein and N. Georgiadis. Spatial statistics to quantify patterns of herd dispersion in a savanna herbivore community. In *Resource Ecology*, volume 23, pages 33–51. Springer Netherlands, 2008.

[26] A. Stein, V. Tolpekin, and O. Spatenkova. The use of statistical point processes in geoinfrmation analysis. In *The Joint International Conference on Theory, Data Handling and Modelling in GeoSpatial Information Science*, volume 38, pages 109–113, 2010.

[27] M. N. M. Van Lieshout. A j-function for inhomogeneous point processes. *Statistica Neerlandica*, 65(2):183–201, 2011.

[28] M. Walessa and M. Datcu. Model-based despeckling and information extraction from SAR images. *IEEE Transactions on geoscience and remote sensing*, 38(5, Part 1):2258–2269, 2000.

[29] C. Walter, A. B. McBratney, R. A. V. Rossel, and J. A. Markus. Spatial point-process statistics: concepts and application to the analysis of lead contamination in urban soil. *Environmetrics*, 16(4):339–355, 2005.

Appendix A

Appendix1

Table A.1 Sumarry of strong reflectors

Summary of forest area corner reflectors			
Statistics	X	Y	Intensity
Min.	1.5	7.5	59005
1st Qu.	20.5	12.5	64080
Median	47.5	79.5	85201
Mean	50.2	57.8	115612
3rd Qu.	79.5	89.5	115839
Max	88.5	94.5	520173

Summary of agricultural area corner reflectors			
Statistics	X	Y	Intensity
Min.	0.5	1.5	70885
1st Qu.	26.5	49.5	80952
Median	52.5	74.5	97122
Mean	50.1	63.74	139680
3rd Qu.	70.5	85.5	131114
Max	99.5	99.5	1225268

Summary of urban area corner reflectors			
Statistics	X	Y	Intensity
Min.	0.5	0.5	93236
1st Qu.	25.5	34.5	119751
Median	57.5	66.5	161046
Mean	53.22	59.66	353506
3rd Qu.	78.5	82.5	276429
Max	99.5	99.5	10800000

Table A.2 Bright speckled pixels of forest area

X	Y	Intensity	X	Y	Intensity	X	Y	Intensity
70.5	48.5	58079.03	21.5	86.5	49730.55	87.5	31.5	45306.82
8.5	82.5	57901.75	28.5	43.5	49071.02	95.5	85.5	45208.86
18.5	73.5	57723.11	99.5	13.5	48900.56	56.5	37.5	45153.22
7.5	81.5	56910.93	91.5	68.5	48720.09	21.5	98.5	45118.54
19.5	85.5	56488.31	62.5	70.5	48660.76	31.5	22.5	45087.06
20.5	86.5	56379.47	95.5	67.5	48556.76	20.5	85.5	45060.27
45.5	19.5	55918.03	79.5	13.5	48526.93	35.5	18.5	44969.77
2.5	27.5	54922.11	2.5	28.5	48402.27	20.5	95.5	44915.88
20.5	71.5	54850.19	97.5	33.5	48385.88	93.5	86.5	44790.07
70.5	99.5	54479.95	96.5	5.5	48378.72	99.5	62.5	44782.84
80.5	12.5	54466.85	78.5	94.5	48139.02	51.5	72.5	44737.52
79.5	93.5	54347.75	45.5	61.5	48111.57	72.5	47.5	44622.67
36.5	7.5	53566.91	99.5	55.5	47842.81	11.5	94.5	44585.13
80.5	10.5	53391.72	22.5	96.5	47796.75	41.5	87.5	44423.20
2.5	7.5	53320.14	48.5	51.5	47554.58	80.5	11.5	44251.04
20.5	4.5	53293.38	61.5	55.5	47476.82	81.5	35.5	44170.68
60.5	61.5	53263.59	99.5	61.5	47464.82	95.5	32.5	44100.47
97.5	5.5	52764.00	66.5	72.5	46793.88	83.5	19.5	44013.25
59.5	73.5	52376.29	87.5	10.5	46602.41	30.5	10.5	43957.28
51.5	57.5	52037.22	69.5	7.5	46550.53	52.5	83.5	43923.09
5.5	90.5	51361.35	19.5	94.5	46424.32	19.5	73.5	43897.12
78.5	11.5	51029.50	2.5	45.5	46358.41	46.5	87.5	43856.39
82.5	58.5	50894.62	89.5	10.5	46315.15	98.5	85.5	43746.65
46.5	52.5	50789.79	60.5	82.5	46275.94	62.5	55.5	43727.31
68.5	73.5	50619.36	6.5	68.5	46274.57	22.5	98.5	43724.19
46.5	76.5	50593.81	46.5	53.5	46217.31	6.5	50.5	43716.90
88.5	64.5	50494.75	13.5	16.5	46176.39	64.5	59.5	43662.98
78.5	13.5	50474.30	17.5	52.5	45989.15	92.5	68.5	43632.82
97.5	2.5	50143.03	60.5	74.5	45920.31	88.5	9.5	43606.20
65.5	68.5	49952.50	80.5	93.5	45890.30	28.5	62.5	43597.67
3.5	94.5	49907.00	91.5	58.5	45882.25	8.5	19.5	43503.22
19.5	66.5	49841.50	72.5	57.5	45856.02	41.5	15.5	43487.33
46.5	19.5	49738.97	3.5	30.5	45732.07			
46.5	61.5	49734.40	92.5	58.5	45423.87			

Table A.3 Bright speckled pixels of agricultural area

X	Y	Intensity	X	Y	Intensity	X	Y	Intensity
45.5	88.5	70814.92	81.5	97.5	67228.13	14.5	12.5	64783.38
32.5	96.5	70021.88	6.5	59.5	67221.20	66.5	95.5	64686.86
85.5	2.5	69919.81	82.5	90.5	67148.76	63.5	50.5	64569.65
27.5	12.5	69906.33	62.5	85.5	67074.62	54.5	74.5	64564.22
79.5	87.5	69781.85	26.5	92.5	67061.93	21.5	32.5	64351.32
18.5	78.5	69727.97	91.5	58.5	67057.54	8.5	52.5	64339.63
20.5	11.5	69671.59	62.5	91.5	67011.05	57.5	76.5	64263.02
25.5	92.5	69393.42	67.5	93.5	66973.83	73.5	91.5	64095.68
65.5	60.5	69242.89	65.5	93.5	66915.56	94.5	41.5	64088.56
43.5	53.5	69183.10	46.5	38.5	66903.39	19.5	79.5	64038.42
30.5	93.5	69142.91	20.5	92.5	66705.98	74.5	17.5	63951.94
45.5	84.5	69096.60	73.5	88.5	66649.02	54.5	81.5	63916.41
46.5	42.5	69002.49	22.5	75.5	66634.13	21.5	92.5	63845.45
68.5	8.5	68840.82	3.5	14.5	66532.91	10.5	75.5	63783.81
80.5	88.5	68767.53	84.5	75.5	66396.19	93.5	39.5	63738.01
5.5	57.5	68586.36	69.5	7.5	66365.95	21.5	3.5	63648.88
75.5	89.5	68553.31	69.5	11.5	66216.88	14.5	83.5	63519.97
13.5	76.5	68291.42	65.5	86.5	66174.55	45.5	98.5	63447.34
51.5	43.5	68275.20	53.5	23.5	66140.06	49.5	85.5	63230.68
13.5	78.5	68247.16	0.5	62.5	65905.70	14.5	13.5	63222.64
16.5	84.5	67965.59	44.5	51.5	65580.91	78.5	66.5	63196.77
20.5	31.5	67779.52	45.5	86.5	65343.46	48.5	84.5	63058.68
9.5	84.5	67733.09	91.5	90.5	65201.92	19.5	78.5	63044.97
47.5	85.5	67732.81	61.5	48.5	65122.41	70.5	7.5	62888.43
77.5	64.5	67694.90	89.5	75.5	65096.98	7.5	45.5	62887.70
51.5	87.5	67679.26	91.5	1.5	65078.41	11.5	24.5	62804.17
89.5	74.5	67628.98	31.5	9.5	64961.44	77.5	87.5	62787.10
7.5	47.5	67574.08	66.5	94.5	64888.62	19.5	23.5	62634.09
70.5	16.5	67509.08	3.5	94.5	64880.73	81.5	90.5	62632.54
9.5	75.5	67402.59	49.5	79.5	64840.40	17.5	10.5	62589.70
53.5	82.5	67301.09	38.5	22.5	64829.02	12.5	79.5	62503.56
62.5	82.5	67281.05	52.5	22.5	64800.46			
23.5	27.5	67236.63	5.5	97.5	64800.15			

Table A.4 Bright speckled pixels of urban area

X	Y	Intensity	X	Y	Intensity	X	Y	Intensity
68.5	76.5	93168.77	4.5	57.5	90266.75	18.5	72.5	87180.10
4.5	82.5	93097.16	61.5	82.5	90067.05	1.5	85.5	87175.51
84.5	59.5	92963.84	62.5	97.5	89946.53	54.5	8.5	87061.90
85.5	88.5	92953.69	57.5	50.5	89906.62	22.5	6.5	87022.01
39.5	14.5	92738.38	15.5	65.5	89841.81	94.5	46.5	86836.29
72.5	58.5	92732.56	94.5	42.5	89802.98	72.5	79.5	86778.25
24.5	80.5	92731.73	76.5	10.5	89719.28	24.5	16.5	86524.58
90.5	27.5	92563.68	63.5	66.5	89697.47	12.5	65.5	86405.71
99.5	32.5	92548.98	53.5	1.5	89546.52	11.5	24.5	86401.72
41.5	87.5	92508.23	77.5	53.5	89346.48	95.5	81.5	86362.80
63.5	15.5	92506.52	78.5	78.5	89273.29	27.5	58.5	86246.78
83.5	81.5	92411.15	96.5	40.5	89100.11	55.5	27.5	86114.70
84.5	82.5	91912.78	88.5	61.5	88865.88	61.5	0.5	86025.88
22.5	71.5	91825.82	9.5	30.5	88848.95	91.5	41.5	85889.66
85.5	16.5	91623.69	52.5	51.5	88796.48	67.5	72.5	85812.63
58.5	67.5	91483.45	59.5	96.5	88785.61	94.5	87.5	85663.48
32.5	78.5	91482.05	61.5	61.5	88724.31	40.5	80.5	85292.13
19.5	73.5	91305.09	55.5	1.5	88657.06	56.5	94.5	85233.99
19.5	10.5	91152.75	66.5	94.5	88653.14	55.5	99.5	85207.09
30.5	13.5	91133.70	99.5	11.5	88651.56	46.5	20.5	85184.07
95.5	23.5	91115.88	91.5	30.5	88504.89	49.5	79.5	85023.79
23.5	41.5	91053.57	93.5	42.5	88325.42	88.5	56.5	84986.28
95.5	55.5	90993.13	22.5	68.5	88293.73	62.5	17.5	84595.69
43.5	44.5	90662.66	56.5	72.5	88247.99	64.5	67.5	84551.17
76.5	53.5	90641.70	71.5	48.5	88015.23	55.5	93.5	84336.77
78.5	79.5	90640.89	60.5	95.5	87873.32	55.5	13.5	84255.02
0.5	29.5	90582.14	29.5	58.5	87660.40	94.5	47.5	84243.17
99.5	40.5	90563.64	66.5	90.5	87448.40	71.5	60.5	84239.13
71.5	83.5	90529.01	8.5	27.5	87426.67	6.5	40.5	84236.47
93.5	55.5	90421.21	67.5	79.5	87333.84	18.5	70.5	84234.89
85.5	4.5	90419.44	67.5	75.5	87232.36	64.5	90.5	84060.22

Table A.5 Summary of bright speckled pixels

Summary of bright speckled pixels of forest area			
Statistics	X	Y	Intensity
Min.	2.50	2.50	43487
1st Qu.	21.25	21.75	44956
Median	58.00	58.50	47471
Mean	53.81	53.64	48258
3rd Qu.	80.75	77.75	50600
Max.	99.50	99.50	58079

Summary of brigh speckled pixels of agriculture area			
Statistics	X	Y	Intensity
Min.	0.50	1.50	62504
1st Qu.	19.50	38.50	64263
Median	47.50	75.50	66366
Mean	45.98	61.87	66122
3rd Qu.	69.50	87.50	67695
Max	94.50	98.50	70815

Summary of bright speckled pixels of urban area			
Statistics	X	Y	Intensity
Min.	0.50	0.50	84060
1st Qu.	32.50	30.50	86406
Median	61.50	58.50	88786
Mean	57.87	54.66	88694
3rd Qu.	83.50	79.50	90663
Max.	99.50	99.50	93169

Table A.6 Dark speckled pixels of forest area

X	Y	Intensity	X	Y	Intensity	X	Y	Intensity
33.5	66.5	801.33	0.5	81.5	2635.47	48.5	49.5	3072.63
32.5	6.5	1110.98	60.5	33.5	2644.81	73.5	13.5	3089.23
58.5	89.5	1224.97	6.5	87.5	2649.29	22.5	87.5	3096.39
85.5	33.5	1636.76	46.5	32.5	2656.28	65.5	50.5	3113.03
41.5	70.5	1772.71	83.5	50.5	2659.39	9.5	85.5	3121.65
51.5	40.5	1799.50	6.5	86.5	2660.14	35.5	82.5	3143.40
40.5	70.5	1884.32	12.5	78.5	2664.40	18.5	47.5	3155.06
6.5	46.5	2001.58	86.5	96.5	2669.50	85.5	25.5	3168.68
99.5	74.5	2079.83	48.5	12.5	2688.25	71.5	23.5	3173.96
57.5	61.5	2086.18	33.5	67.5	2690.94	16.5	63.5	3178.79
1.5	80.5	2092.53	55.5	88.5	2705.13	75.5	62.5	3191.68
33.5	81.5	2106.16	89.5	16.5	2720.43	82.5	96.5	3198.43
6.5	70.5	2111.95	62.5	94.5	2755.06	66.5	44.5	3202.69
35.5	25.5	2122.72	44.5	73.5	2761.13	43.5	4.5	3206.70
5.5	37.5	2147.84	6.5	67.5	2767.51	11.5	88.5	3208.34
59.5	30.5	2179.67	75.5	45.5	2770.17	85.5	27.5	3215.69
46.5	6.5	2210.65	72.5	75.5	2780.67	46.5	43.5	3217.57
19.5	11.5	2240.50	31.5	97.5	2788.70	35.5	67.5	3219.42
4.5	57.5	2283.57	98.5	75.5	2793.50	27.5	9.5	3247.86
34.5	66.5	2307.70	50.5	9.5	2832.41	81.5	96.5	3255.62
84.5	50.5	2399.89	0.5	78.5	2853.50	50.5	34.5	3257.12
32.5	44.5	2403.10	14.5	86.5	2867.20	34.5	62.5	3270.57
84.5	48.5	2409.56	19.5	62.5	2902.13	42.5	28.5	3271.36
83.5	96.5	2409.85	35.5	65.5	2913.35	72.5	92.5	3273.71
34.5	67.5	2450.96	11.5	89.5	2936.57	74.5	13.5	3284.05
10.5	77.5	2463.74	91.5	49.5	2950.51	60.5	35.5	3293.79
0.5	85.5	2471.39	7.5	2.5	2951.54	33.5	69.5	3296.87
52.5	88.5	2494.86	9.5	9.5	2970.79	37.5	63.5	3300.68
5.5	82.5	2525.79	16.5	35.5	3011.31	70.5	27.5	3304.79
28.5	65.5	2541.22	12.5	49.5	3012.59	57.5	89.5	3314.65
34.5	81.5	2573.46	54.5	11.5	3022.14	74.5	88.5	3326.20
83.5	70.5	2597.64	52.5	0.5	3037.65	9.5	14.5	3327.09
17.5	36.5	2602.39	34.5	48.5	3045.64			
13.5	85.5	2602.77	97.5	80.5	3066.29			

Table A.7 Dark speckled pixels of agricultural area

X	Y	Intensity	X	Y	Intensity	X	Y	Intensity
59.5	90.5	1471.39	36.5	88.5	2422.06	90.5	25.5	2851.82
8.5	71.5	1476.40	37.5	40.5	2431.08	51.5	63.5	2866.58
48.5	70.5	1482.83	42.5	74.5	2463.83	10.5	2.5	2882.84
23.5	80.5	1508.49	85.5	26.5	2467.84	98.5	19.5	2890.41
7.5	81.5	1521.36	34.5	76.5	2469.83	60.5	29.5	2923.63
47.5	21.5	1646.10	90.5	6.5	2472.43	32.5	73.5	2929.25
74.5	51.5	1656.20	74.5	64.5	2492.79	58.5	30.5	2955.38
49.5	99.5	1721.94	76.5	34.5	2504.79	18.5	70.5	2964.37
35.5	38.5	1737.51	77.5	32.5	2538.62	88.5	54.5	2974.80
30.5	80.5	1818.68	7.5	72.5	2555.23	18.5	68.5	2975.92
17.5	67.5	1822.73	96.5	36.5	2561.21	16.5	65.5	2986.27
79.5	44.5	1888.91	22.5	65.5	2562.43	0.5	43.5	3004.26
5.5	12.5	1916.34	86.5	6.5	2573.12	36.5	37.5	3028.12
51.5	98.5	1952.92	20.5	70.5	2576.69	83.5	61.5	3030.50
78.5	19.5	1957.79	88.5	57.5	2592.36	66.5	80.5	3033.85
18.5	62.5	1990.00	37.5	85.5	2615.50	61.5	77.5	3040.94
88.5	62.5	1990.80	76.5	81.5	2623.87	48.5	60.5	3058.45
48.5	19.5	2001.99	84.5	4.5	2640.99	35.5	12.5	3065.62
32.5	84.5	2051.59	29.5	84.5	2687.58	88.5	34.5	3068.08
32.5	4.5	2120.36	77.5	33.5	2688.25	39.5	40.5	3075.90
20.5	64.5	2121.21	45.5	23.5	2693.47	3.5	76.5	3077.74
30.5	84.5	2129.31	6.5	11.5	2700.14	22.5	86.5	3086.78
38.5	82.5	2134.98	74.5	37.5	2700.27	35.5	56.5	3088.94
75.5	35.5	2153.27	60.5	57.5	2724.51	51.5	57.5	3089.59
19.5	67.5	2242.59	16.5	64.5	2756.91	80.5	41.5	3115.25
35.5	75.5	2246.64	4.5	76.5	2763.51	91.5	55.5	3126.97
31.5	84.5	2246.66	14.5	90.5	2768.33	91.5	83.5	3145.62
0.5	71.5	2309.89	38.5	67.5	2774.14	49.5	56.5	3154.40
16.5	66.5	2312.15	79.5	36.5	2791.67	20.5	67.5	3194.25
33.5	74.5	2315.96	39.5	62.5	2796.27	35.5	82.5	3197.04
19.5	70.5	2370.06	18.5	66.5	2816.94	58.5	28.5	3197.36
48.5	10.5	2371.54	2.5	76.5	2838.50			
23.5	24.5	2408.99	84.5	61.5	2842.41			

Table A.8 Dark speckled pixels of urban area

X	Y	Intensity	X	Y	Intensity	X	Y	Intensity
7.5	51.5	1491.24	29.5	38.5	3131.86	84.5	19.5	3691.11
74.5	77.5	1896.73	3.5	91.5	3178.38	38.5	89.5	3697.61
17.5	0.5	2106.59	83.5	90.5	3178.67	88.5	9.5	3708.84
16.5	0.5	2219.04	42.5	30.5	3202.85	7.5	4.5	3737.08
7.5	17.5	2243.15	98.5	72.5	3219.35	86.5	50.5	3745.49
3.5	93.5	2252.57	75.5	93.5	3221.35	4.5	1.5	3754.02
60.5	23.5	2320.23	78.5	98.5	3290.77	72.5	44.5	3761.51
9.5	61.5	2403.95	32.5	34.5	3317.00	33.5	35.5	3774.59
3.5	92.5	2446.90	50.5	18.5	3323.43	95.5	26.5	3781.76
23.5	48.5	2460.77	61.5	88.5	3328.97	75.5	14.5	3795.21
74.5	86.5	2490.02	39.5	45.5	3329.32	7.5	70.5	3817.21
59.5	58.5	2588.33	31.5	37.5	3354.66	22.5	42.5	3823.69
22.5	95.5	2605.68	61.5	89.5	3416.43	87.5	86.5	3827.88
21.5	66.5	2640.02	22.5	14.5	3434.67	37.5	45.5	3836.57
35.5	72.5	2689.36	4.5	70.5	3446.34	79.5	93.5	3840.50
61.5	52.5	2703.29	1.5	61.5	3446.45	76.5	38.5	3846.62
0.5	57.5	2706.02	0.5	74.5	3485.97	8.5	86.5	3850.59
58.5	59.5	2759.19	55.5	36.5	3496.69	94.5	11.5	3863.52
30.5	28.5	2766.42	62.5	48.5	3531.26	47.5	70.5	3873.77
83.5	17.5	2775.88	38.5	48.5	3540.46	77.5	45.5	3878.28
36.5	45.5	2797.62	37.5	44.5	3553.71	11.5	13.5	3881.81
38.5	45.5	2806.90	72.5	32.5	3557.87	25.5	23.5	3888.40
20.5	14.5	2837.87	57.5	19.5	3560.54	85.5	53.5	3889.82
99.5	23.5	2861.32	87.5	9.5	3574.90	71.5	34.5	3894.81
35.5	46.5	2891.67	12.5	96.5	3608.92	25.5	64.5	3901.53
7.5	93.5	2929.68	76.5	42.5	3610.07	6.5	93.5	3902.66
26.5	23.5	2953.47	88.5	74.5	3616.47	33.5	31.5	3906.28
0.5	64.5	2989.97	8.5	94.5	3620.30	92.5	98.5	3908.19
76.5	41.5	3009.89	31.5	28.5	3625.51	27.5	77.5	3919.11
60.5	22.5	3088.40	31.5	29.5	3667.16	33.5	95.5	3923.92
2.5	95.5	3097.68	28.5	49.5	3686.14	76.5	44.5	3927.17

Table A.9 Summary of dark speckles

Summary of dark speckled pixels of forest area			
Statistics	X	Y	Intensity
Min.	0.50	0.50	801
1st Qu.	17.50	34.25	2461
Median	41.00	63.00	2775
Mean	43.71	56.40	2720
3rd Qu.	67.50	81.50	3159
Max.	99.50	97.50	3327

Summary of dark speckled pixels of agricultural area			
Statistics	X	Y	Intensity
Min.	0.50	2.50	1471
1st Qu.	20.50	35.50	2243
Median	38.50	62.50	2616
Mean	45.83	55.61	2537
3rd Qu.	74.50	75.50	2955
Max.	98.50	99.50	3197

Summary of dark speckled pixels of urban area			
Statistics	X	Y	Intensity
Min.	0.50	0.50	1491
1st Qu.	20.50	28.50	2861
Median	37.50	46.50	3446
Mean	44.07	51.63	3293
3rd Qu.	74.50	74.50	3775
Max.	99.50	98.50	3927

Appendix A

Appendix2

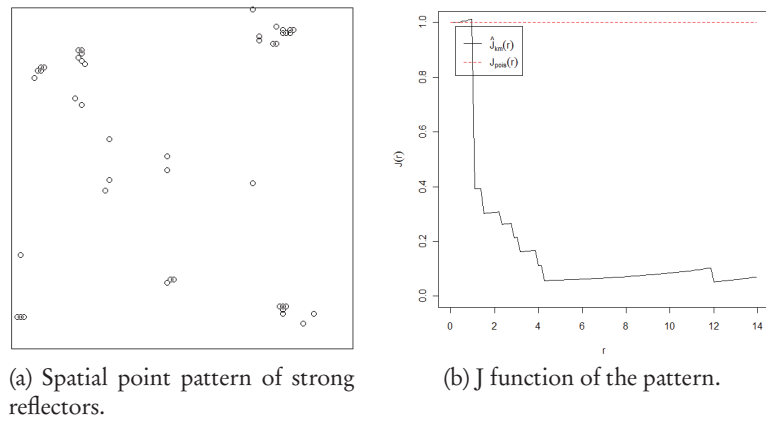(a) Spatial point pattern of strong reflectors.

(b) J function of the pattern.

Figure A.1: Spatial point pattern of strong reflectors in forest area and J function of the pattern based on analysis ENL value 5.

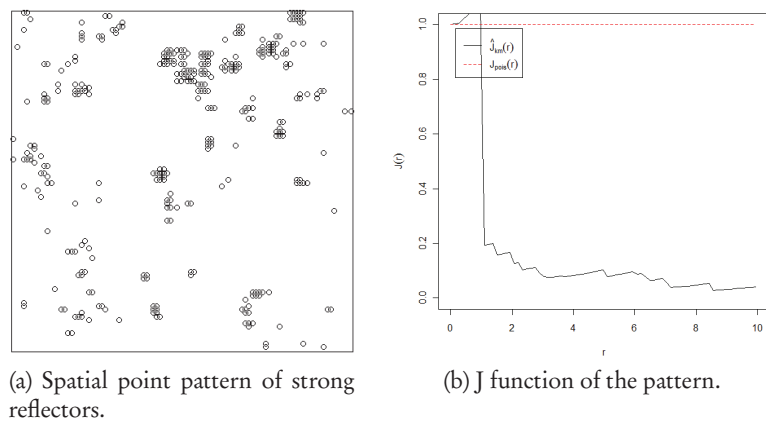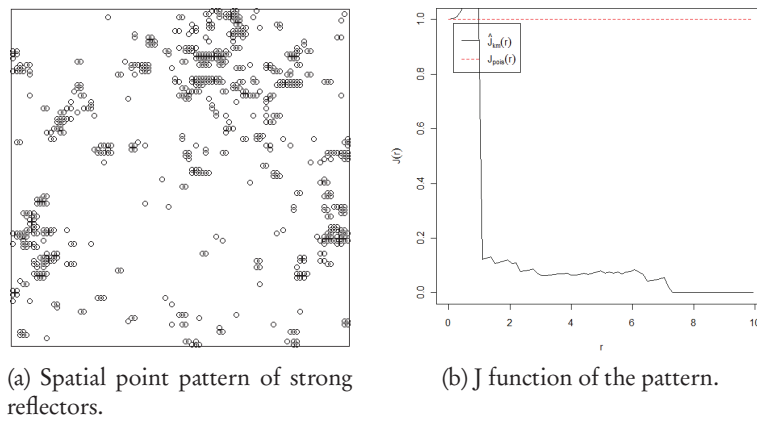(a) Spatial point pattern of strong reflectors.

(b) J function of the pattern.

Figure A.2: Spatial point pattern of strong reflectors in agricultural area and J function of the pattern based on analysis ENL value 5.

(a) Spatial point pattern of strong reflectors.

(b) J function of the pattern.

Figure A.3: Spatial point pattern of strong reflectors in urban area and J function of the pattern based on analysis ENL value 5.

(a) Spatial point pattern of speckles.

(b) Intensity map of the pattern.
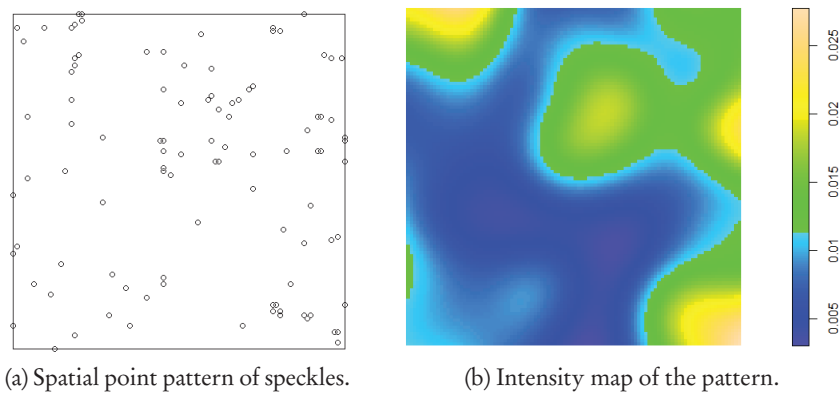
Figure A.4: Spatial point pattern of speckles in forest area and Intensity map of the pattern based on analysis ENL value 5.
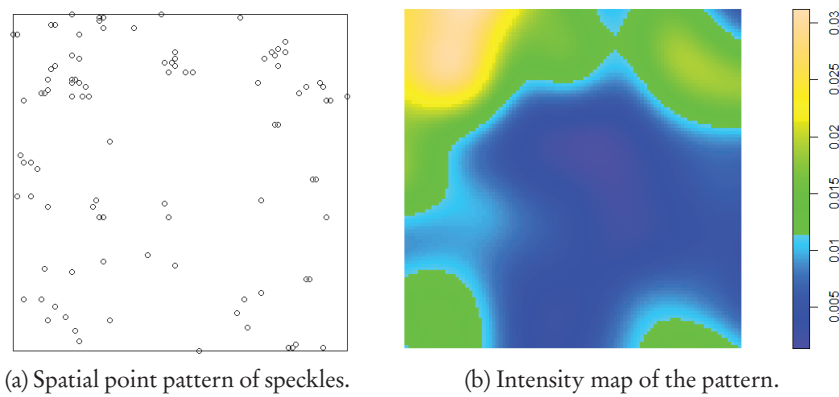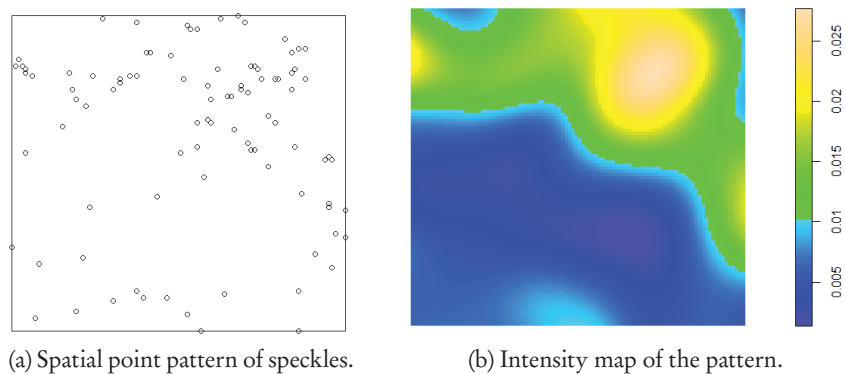

(a) Spatial point pattern of speckles.

(b) Intensity map of the pattern.

Figure A.5: Spatial point pattern of speckles in agricultural area and Intensity map of the pattern based on analysis ENL value 5.

(a) Spatial point pattern of speckles.

(b) Intensity map of the pattern.

Figure A.6: Spatial point pattern of speckles in urban area and Intensity map of the pattern based on analysis ENL value **5**.

(a) F function
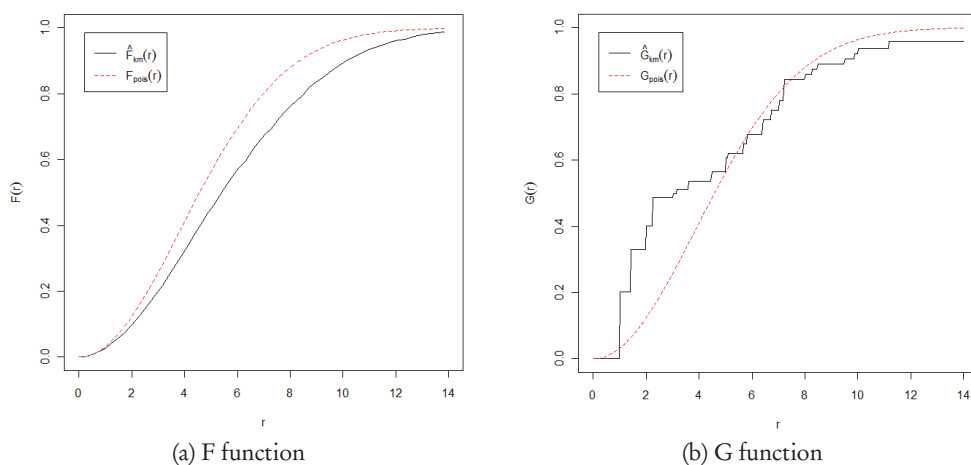
(b) G function

Figure A.7: F and G functions of speckles in forest area based on analysis ENL value **5**.

(a) J function
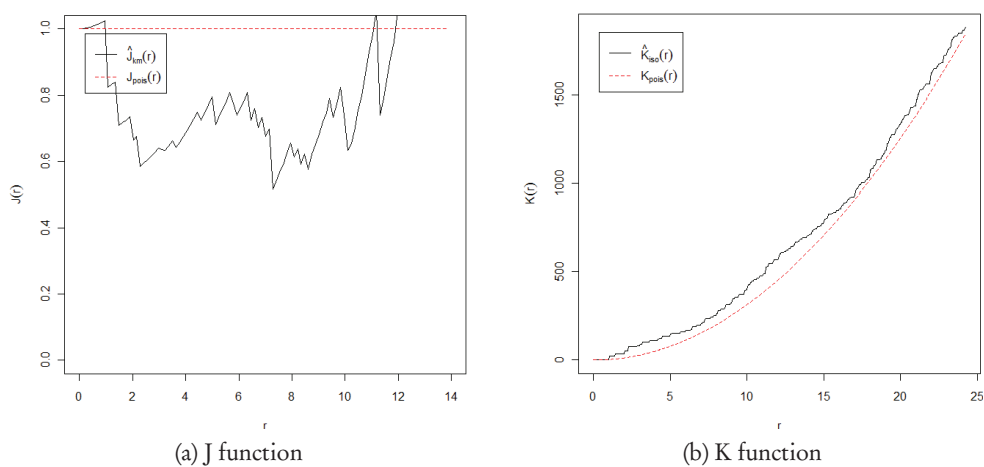
(b) K function

Figure A.8: J and K functions of speckles in forest area based on analysis ENL value **5**.

(a) F function
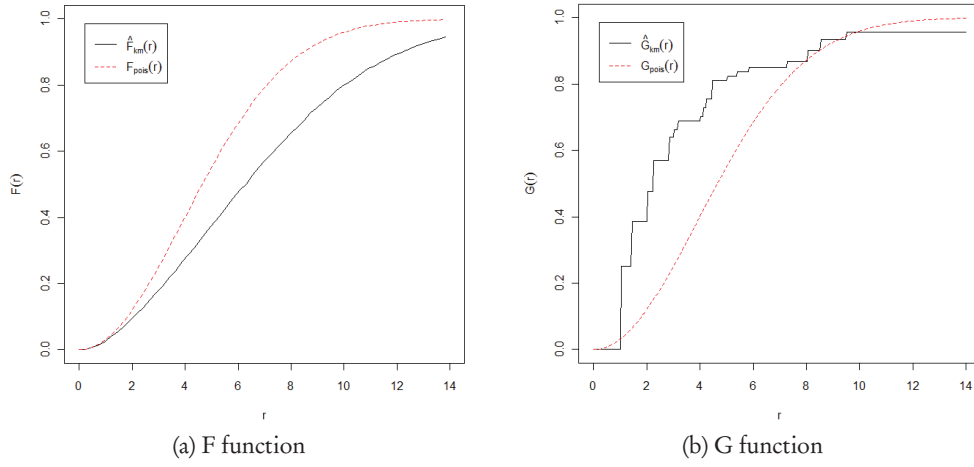
(b) G function

Figure A.9: F and G functions of speckles in agricultural area based on analysis ENL value 5.

(a) J function
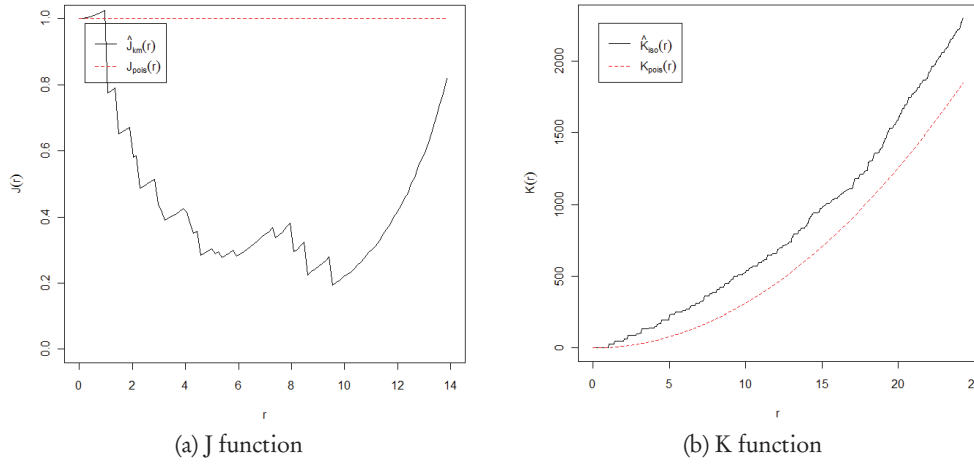
(b) K function

Figure A.10: J and K functions of speckles in agricultural area based on analysis ENL value 5.

(a) F function
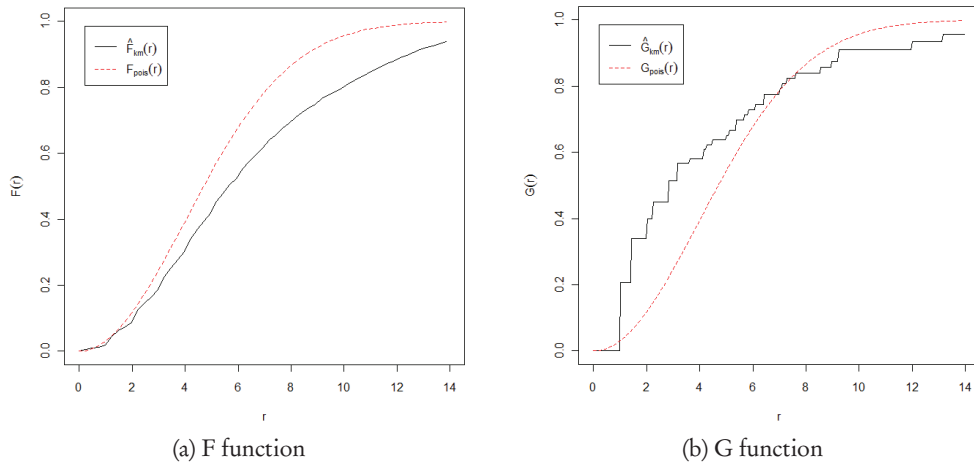
(b) G function

Figure A.11: F and G functions of speckles in urban area based on analysis ENL value 5.

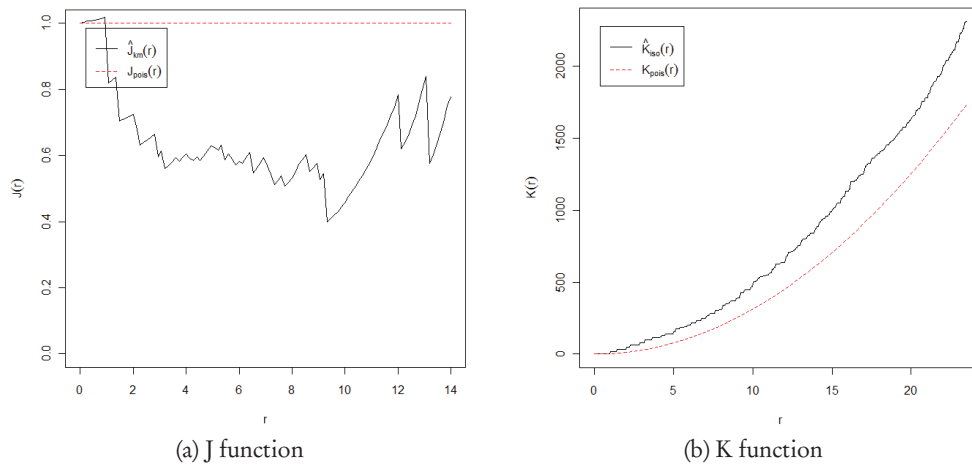(a) J function

(b) K function

Figure A.12: J and K functions of speckles in urban area based on analysis ENL value 5.